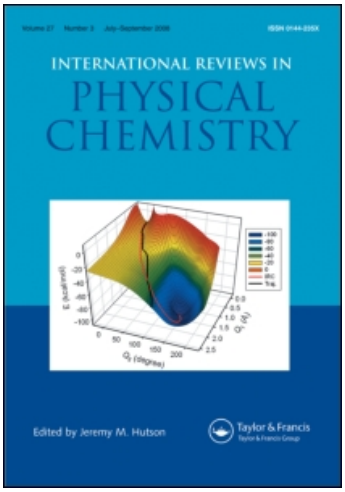

International Reviews in Physical Chemistry
Publication details, including instructions for authors and subscription information:
http://www.informaworld.com/smpp/title~content=t713724383

Application of ion chemistry and the SIFT technique to the quantitative analysis of trace gases in air and on breath

David Smith[a]; Patrik Španěl[a]
[a] Department of Biomedical Engineering and Medical Physics, Hospital Centre, University of Keele, Stoke-on-Trent, Staffs, UK

To cite this Article Smith, David and Španěl, Patrik(1996) 'Application of ion chemistry and the SIFT technique to the quantitative analysis of trace gases in air and on breath', International Reviews in Physical Chemistry, 15: 1, 231 — 271
To link to this Article: DOI: 10.1080/01442359609353183
URL: http://dx.doi.org/10.1080/01442359609353183

INTERNATIONAL REVIEWS IN PHYSICAL CHEMISTRY, 1996, VOL. 15, NO. 1, 231–271

Application of ion chemistry and the SIFT technique to the quantitative analysis of trace gases in air and on breath

by DAVID SMITH and PATRIK ŠPANĚL

Department of Biomedical Engineering and Medical Physics, Hospital Centre, University of Keele, Thornburrow Drive, Hartshill, Stoke-on-Trent, Staffs ST4 7QB, UK

Our major objective in this paper is to describe a new method we have developed for the analysis of trace gases at partial pressures down to the ppb level in atmospheric air, with special emphasis on the detection and quantification of trace gases on human breath. It involves the use of our selected ion flow tube (SIFT) technique which we previously developed and used extensively for the study of gas phase ionic reactions occurring in ionized media such as the terrestrial atmosphere and interstellar gas clouds. Before discussing this analytical technique we describe the results of our very recent SIFT and flowing afterglow (FA) studies of the reactions of the H_3O^+ and OH^- ions, of their hydrates $H_3O^+(H_2O)_{1,2,3}$ and $OH^-(H_2O)_{1,2}$, and of NO^+ and O_2^+, with several hydrocarbons and oxygen-bearing organic molecules, studies that are very relevant to our trace gas analytical studies. Then follows a detailed discussion of the application of our SIFT technique to trace gas analysis, after which we present some results obtained for the analyses of laboratory air, the breath of a healthy non-smoking person, the breath of a person who regularly smokes cigarettes, the complex vapours emitted by banana and onion, and the molecules present in a butane/air flame. We show how the quantitative analysis of breath can be achieved from only a single exhalation and in real time (the time response of the instrument is only about 20 ms). We also show how the time variation of breath gases over long time periods can be followed, using the decay of ethanol on the breath after the ingestion of distilled liquor as an example, yet simultaneously following several other trace gases including acetone and isoprene which are very easily detected on the breath of all individuals because of their relatively high partial pressures (typically 100 to 1000 ppb). The breath of a smoker is richer in complex molecules, some nitrogen containing organics apparently being very evident at the 5 to 50 ppb level. These results and those for banana and onion vapours and butane/air flame forcibly demonstrate the value and the scope of our SIFT ion chemistry approach to the analysis of very complex gas mixtures, and that this method is accurately quantitative if the appropriate ion chemistry is properly understood.

Foreword

Michael Henchman is a dear and valued friend of us both. One of us (D.S.) has known him for some twenty years, both as a respected colleague and friend, a friendship that began when he spent a very enjoyable and scientifically-profitable sabbatical year at the University of Birmingham in 1980 where we had developed the SIFT and flowing afterglow/Langmuir probe (FALP) techniques. Michael's insight and understanding of ion chemistry brought great stimulus to our work, and especially to the very interesting studies of isotope exchange in ion/neutral reactions, collaborative work which we continue to the present. Michael is an erudite man, with interests and expertise not only in chemistry, but also in art, literature and the theatre. He is also one of the great entertainers, enjoying the preparation of wonderful dinners and then interesting and amusing his guests as part of the very generous efforts he

0144–235X/96 $12·00

invariably makes when one visits his home. Yet his most kindly feature is the loyalty and concern he shows for his friends in times of need; we have been the grateful beneficiaries of this most human of instincts and for this also we are eternally grateful to him. We offer this paper on our latest developments in fundamental and applied ion chemistry with respect and affection towards a fine scientist and a very dear friend as our contribution to Michael's sixtieth birthday celebrations.

1. Introduction

The analysis of complex gas mixtures comprising perhaps dozens and even hundreds of different gases at widely different partial pressures is a very difficult challenge, but one that needs to be tackled if complex systems such as environmental air, human breath, car exhaust gas and the vapours emitted from fruit, to mention a few, are to be accurately analysed. The most widely used and most successful technique that has been used is gas chromatography (see below). Conventional mass spectrometry in which the gas is sampled into an electron impact ion source is very valuable if particular compounds in a simple mixture are to be identified, when the recognition of the 'cracking pattern' can identify the molecules present, but is practically useless for complex mixtures of trace gases. We comment on these problems again later in §3.1. The more recent forms of ion source such as fast atom bombardment sources (which minimize fragmentation of the molecules to be detected) and electrospray methods, have been successful in the characterisation of large molecules, but are not suitable for the analysis of gas mixtures. Some recent clever mass spectrometric innovations are reported in two recent special journal issues devoted to mass spectrometry [1, 2].

Chemical ionization in which the ionization of the molecules is achieved by 'soft ionization' using ions was investigated many years ago [3]. The introduction of, for example, methane into an electron impact ion source along with the gas to be analysed first produces protonated methane ions by ion–molecule reactions and then protons are transferred from these precursor CH_5^+ ions to the molecules to be detected, M. The mass spectrometer then detects the product MH^+ ions. This technique minimizes the fragmentation of the proton acceptor molecules, M, and thus simplifies the subsequent mass spectrum *vis-à-vis* that produced by electron impact. However, this technique has only been used for very simple mixtures and there are potential complications due to unknown ion chemistry that can occur in an active ion source; this then is not a useful way of quantitatively analysing complex gas mixtures.

A desirable approach is to first separate the precursor ions from the complex mixture of ions in the source and then use them in a more controlled fashion to ionize the molecules in the mixture. Now the choice of the precursor ions is important; and as we will show below, H_3O^+ ions have some very important advantages for the analysis of the trace gases in air and on breath, but they are by no means the only useful ions. We will also show that O_2^+ ions are very useful for this purpose. Ultimately, the most useful precursor ion depends on the properties (e.g. the ionization potential, the proton affinity) of the molecules to be detected.

It is obviously desirable when detecting trace gases in air to be able to discriminate against the major air components, e.g. N_2. This has been achieved previously [4] by using the rare gas ions Kr^+ and Xe^+. These ions undergo charge transfer reactions with most gases that have ionization energies lower than Kr and Xe atoms (significantly not so for N_2) [5, 6] and as such they are useful in the analysis of modified air such as car

exhaust gases [4]. This is the basis of a very successful commercial ion beam device [7], in which Kr^+ or Xe^+ ions are injected into an octopole ion guide into which is introduced (at low pressure) a sample of the gas mixture to be analysed. Single collisions between the injected ions and the molecular components, M, of the gas mixture result in charge transfer, thus producing only M^+ ions, and the subsequent quantitative mass analysis of the ionic components of the octopole ion guide indicates the molecular components of the gas mixture and their partial pressures. Using this technique, some organic impurities in air down to the 50 ppb level can be detected and quantified. An essential requirement is a library of the rate coefficients and the ionic products for the reactions of Kr^+ and Xe^+ ions with a wide range of molecular gases; this is provided largely by selected ion flow tube (SIFT) [5, 6, 8] and other studies of these reactions [9]. Clearly, this method is not limited to the use of the above precursor ions; ions of even lower ionization energy can be used to achieve further discrimination, and Hg^+ ions are now being used (J. Villinger, private communication).

Our recent contribution to this science has been stimulated largely by our growing interest in the clinical diagnostic value of the identification and quantification of the trace gases on human breath, of the environmental and health aspects of air pollution, and the vapours emitted by various fruits, meats and other food products, not to mention a long-standing interest in combustion chemistry. Our very recent, initial investigations of these will be described later and some interesting data will be presented. In considering the general problem of trace gas analysis in air, especially on breath, we turned our attention back to the proton transfer process previously referred to, as potentially a most profitable soft ionization method, whilst recognising that the separation of the precursor protonated ions from the ion source gas(es) from which they are generated is a vital requirement for accurate quantitative analysis of complex mixtures. This separation requirement immediately invoked our SIFT technique [8] (which we describe in §3.2). Thus we have combined the SIFT technique and the proton transfer process for the analysis of the trace gases in complex gas mixtures, currently achieving a lower limit of sensitivity of about 30 ppb in air and human breath with a very rapid time response, and a significantly lower limit for long sampling times (see later examples in §4). As is explained below, we have greatly exploited the hydronium ion, H_3O^+, as the precursor ion for the ionization of the components of the gas mixtures, principally because it is relatively unreactive with the major components of atmospheric air and of human breath. However, an important point to realize is that H_3O^+ ions undergo three-body association reactions with H_2O molecules when the ambient gas pressure is sufficiently high, and so inevitably when H_3O^+ ions are used for the chemical ionization of gas mixtures containing water vapour (such as atmospheric air and especially human breath) then water cluster ions of the kind $H_3O^+(H_2O)_{1,2,3}$ are present in the gas at some concentrations (but their fraction can be minimized if required, but at the cost of lower sensitivity; see §3), and so the reactions of these cluster ions must be taken into account when performing the analysis of the trace gases in the mixture. Thus, we have thus carried out a detailed study of the reactions of H_3O^+ ions [10] and the cluster ions $H_3O^+(H_2O)_{1,2,3}$ [11] with several gases using our SIFT apparatus in order to provide the required critical kinetic data to support our development of our trace gas analysis technique, and additionally to provide further insight into the proton transfer process and the 'switching reactions' of water cluster ions. Further to these studies, we have carried out a study of the reactions of the negative ions OH^- and $OH^-(H_2O)_{1,2}$ using our flowing afterglow (FA) apparatus to also explore the potential of these as chemical ionization precursor ions

for trace gas analysis [10, 11], and also carried out a SIFT study of the reactions of NO^+ and O_2^+ ions with several organic vapours [12] for the same reasons. As we will indicate later, these last two ionic species do not react rapidly with the major atmospheric gases either, and as such they are potentially valuable for trace gas analysis. As we will indicate, O_2^+ is particularly useful when used in combination with H_3O^+ for analysis.

In this paper the major objective is to review the results of the aforementioned SIFT and FA studies, and then to present some preliminary data obtained using our SIFT technique on the trace gas analysis of atmospheric air, of the breath of non-smokers and of smokers, of the vapours emitted by foods (specifically banana and onion), of some specific food flavours, and of the volatile products of a butane/air flame, which very well illustrate the enormous potential of our techniques for the analysis of the trace gases in a variety of gaseous media.

2. Preparatory SIFT and FALP studies for trace gas analysis

2.1. *Notes on the experimental techniques*

The FA [13] and the SIFT [8, 14, 15] techniques have become standard methods for the study of ion–molecule reactions and other reaction processes [16] and so they do not need to be described in detail here; rather the reader is referred to the above references. However, it is necessary to briefly describe the SIFT technique because it helps the understanding of how we use it for trace gas analysis. Reactant ions are generated in some form of ion source (figure 1), passed through a quadruple mass filter to select ions of a given mass-to-charge ratio, and then injected at low energy (to avoid collisional fragmentation) into a fast flowing carrier gas (usually pure helium at a pressure of typically 0·5 torr). The injected ions quickly thermalise to the gas temperature in collisions with the carrier gas atoms and are convected downstream where they are sampled into a differentially-pumped quadruple mass spectrometer via a pinhole orifice. Now reactant gas is introduced at a controlled and measured flow rate into the carrier gas/thermalized ion swarm, and the primary ion and product ion count rates are determined by the downstream detection system for several flow rates of the reactant gas. From such measurements the rate coefficient and the percentage ion product distribution for the ion–molecule reaction can be obtained. The function of the FA experiment is essentially identical, except that the primary reactant ions are not mass selected but rather they are generated in the carrier gas from a suitable source gas which is ionized usually by a local electrical discharge. In the trace gas analysis procedure described later, the reactant gas is replaced by the sample of gas to be analysed, and the observed product ion currents are directly related to the composition of the gas mixture.

The ion source we used in the fundamental SIFT studies and the trace gas analyses described in this paper is worthy of note. For this method of trace gas analysis, large currents of the precursor ions are desirable which are maintained for long periods of time. To generate H_3O^+ we found that a microwave cavity discharge through argon (pressure $\leqslant$ 0·2 torr) with a trace of water was ideal. We also found that appreciable currents of $H_3O^+ \cdot (H_2O)_{1,2,3}$ ions could be injected from this ion source, which allowed the studies of their reactions also in the SIFT. Additionally, the introduction of a small flow of humid atmospheric air directly into the carrier gas in the SIFT converted a fraction of the injected H_3O^+ ions to the hydrated hydronium ions which assisted, in particular, the studies of the $H_3O^+ \cdot (H_2O)_3$ reactions. Only very small currents of these ions could be injected from the ion source into the carrier gas principally because they

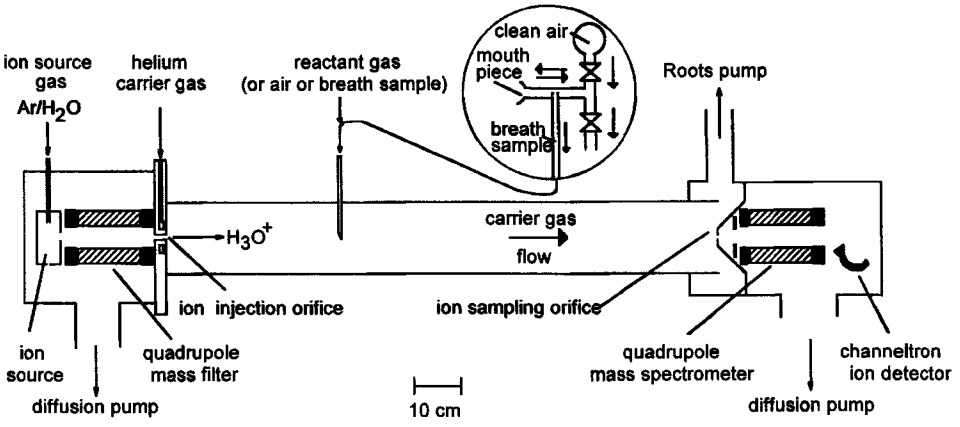

Figure 1. A schematic diagram of the selected ion flow tube (SIFT) apparatus [8] as configured for trace gas analysis, showing the ion source (in this example producing precursor H_3O^+ ions) and the injection quadruple mass filter, the flow tube (length about 100 cm) with the gas sample (air or breath) inlet, and the downstream quadruple mass spectrometer and ion detection system which is used to detect and quantify the ions produced by chemical ionization (proton transfer and switching reactions in this case) of the trace gases in the gas sample. Other precursor ions can be used for the chemical ionization, including NO^+ and O_2^+ (see text).

have to be injected at very low injection energies to inhibit their break-up in collisions with the helium atoms. For our studies of the NO^+ and O_2^+ reactions, it was merely necessary to introduce a trace of an N_2/O_2 mixture into the argon microwave discharge to obtain a rich source of these ions.

We could not obtain adequate currents of $OH^-\cdot(H_2O)_{0,1,2}$ ions from the SIFT microwave discharge ion source and so we used the FA to study the reactions of these ions. Thus, a trace of water vapour was introduced into helium carrier gas upstream of the microwave cavity discharge that formed the flowing afterglow plasma. By carefully limiting the amount of water, essentially OH^- ions only could be obtained; the addition of more water resulted in the production of cluster ions and the fraction of the two hydrates could be varied thus facilitating the determinations of the product ratios for the ion–molecule reactions under study.

The reactant gases and vapours were introduced into the SIFT and FA via mass flow controllers directly from gas cylinders and from above liquids. Then, as mentioned above, the primary reactant ion and product ion count rates were recorded by the downstream mass spectrometer detection system as a function of the reactant gas flow rate, and then the rate coefficients and ion product distributions were determined in the usual way for SIFT and FA experiments [8, 13]. All the measurements referred to in this paper were carried out at a temperature of 300 K. The rate coefficients are considered to be accurate to $\pm 20\%$ when the neutral reactants are permanent gases and $\pm 30\%$ when they are vapours.

2.2. *Reactions of H_3O^+ and OH^- with some hydrocarbons and oxygen-bearing molecules*

The reactions of H_3O^+ and OH^- ions with several hydrocarbons (cyclohexane, methylcyclohexane, cyclopropane, benzene, toluene and isoprene) and several oxygen-bearing organic molecules (methanol, acetaldehyde, ethanol, acetone, diethyl ether,

ethyl acetate, trans 2-hexenal and cis 3-hexenal) were included in this recent study, the H_3O^+ reactions being studied using the SIFT apparatus and the OH^- reactions using the FA apparatus. The detailed results are reported in our recent paper [10], but some of the more interesting results and their relevance to our analytical work are discussed here.

2.2.1. *Reactions of H_3O^+*

When the proton affinity (PA) of an acceptor molecule exceeds that of a protonated donor molecule then proton transfer between these species at thermal energies is expected to be efficient [17], i.e. the measured rate coefficient, k, is expected to be equal to the collisional rate coefficient, k_c [18]. The values of k and k_c are given in table 1 for some representative reactions together with the product ions. PA(H_2O) is 166·5 kcal mol^{-1}, and since the PA of the hydrocarbons cyclopropane, benzene, toluene and isoprene exceed this value, then the k for the reactions of H_3O^+ with these molecules are expected to be equal to their respective k_c as was observed to be so in this study. All four reactions proceed via non-dissociative proton transfer, i.e. only a single product, the protonated molecule, was observed in each reaction, consistent with some previous studies of some of these reactions [19, 20, 21]. For example, the isoprene reaction proceeds thus:

$$H_3O^+ + C_5H_8 \rightarrow C_5H_9^+ + H_2O. \qquad (1)$$

Hence the quantitative detection of these hydrocarbons using H_3O^+ ions is uncomplicated using our SIFT approach described later. However, one of our earlier studies [20] showed that the reaction of H_3O^+ with cyclohexane is very slow, resulting in two products:

$$H_3O^+ + c\text{-}C_6H_{12} \rightarrow C_6H_{11}^+ + H_2 + H_2O \qquad (2a)$$

$$\rightarrow C_6H_{13}^+ + H_2O. \qquad (2b)$$

The branching ratio is about 50% into each channel. On the basis of these observations, together with the reactions of the c-C_6H_{12} with several other ions, we established [20] that PA(c-C_6H_{12}) is 160 kcal mol^{-1}, some 9 kcal mol^{-1} lower than the published value [22]. This reaction, therefore, is of little value for the detection of cyclohexane. In the same manner, the PA of methylcyclohexane was established to be between 164 and 166·5 kcal mol^{-1} in this study [10], i.e. a little lower than that of H_2O.

All eight oxygen-bearing molecules included in this study [10] have large proton affinities [22] and quite large dipole moments [23]. The reactions of both H_3O^+ with all of them were observed to be very fast, the measured k being close to the calculated k_c. The reactions of $H_3O^+$with the majority of these molecules proceed by non-dissociative proton transfer producing only the protonated molecule (thus confirming other results for the methanol [24], acetone, ethanol and acetaldehyde [21] reactions); this facilitates their detection and quantification. An exception is the ethyl acetate reaction in which, in accordance with a previous study [25], a minor second product (of little consequence) appears to be formed:

$$H_3O^+ + CH_3COOC_2H_5 \rightarrow C_4H_9O_2^+ + H_2O \quad (98\%) \qquad (3a)$$

$$\rightarrow C_2H_5O_2^+ + C_2H_4 + H_2O \quad (2\%) \qquad (3b)$$

Very interesting in this group of H_3O^+ reactions from the analytical point of view

Table 1. Kinetic data obtained using the SIFT technique for the reactions of O_2^+ and NO^+ (from [12]), H_3O^+ (from [10]) and $H_3O^+(H_2O)_{1,2,3}$ (from [11]) with the three non-polar hydrocarbons and the three polar oxygen-containing molecules indicated. The measured rate coefficients (in units of 10^{-9} cm^3 s^{-1}) are given for each reaction to the left of each box, and the collisional rate coefficients [18] (in the same units) are given in square brackets to the right. The asterisks associated with the rate coefficients for two NO^+ reactions indicate effective two-body rate coefficients for the three-body association reactions. Also given in each box are the products of the reactions with the percentages in brackets; we designate all the reactant molecules as MH to simplify the product ion designations. If there is only a single product no percentage is given. Below each reactant ion is its recombination energy in electron volts (eV). Associated with each reactant molecule is its ionization energy in eV to the left, its proton affinity in italics given as is conventional in kcal mol^{-1}, and its dipole moment in Debye to the right. This kind of kinetic data are essential for the quantitative analysis of trace gases using our SIFT method. The critical molecular data allow one to judge what reaction processes are energetically possible. Clearly, charge transfer is possible between O_2^+ ions and all the reactant molecules in this table, but for NO^+ this process is only possible in reaction with isoprene and toluene and it is observed. Proton transfer can occur from H_3O^+ to all the reactant molecules except n-pentane because its proton affinity is less than that of H_2O. Note that the H_3O^+ hydrate ions do not react with the non-polar hydrocarbons to produce the water clusters, but the very polar acetone reacts with all three hydrated hydronium ions. For a discussion of this, see text.

Reactant ion RE (eV)	n-pentane $n\text{-}C_5H_{12}$ 10·35, *?* (1·6)	isoprene $CH_2{=}C(CH_3)CH{=}CH_2$ 8·84, *200·4* (0·25)	toluene $c\text{-}C_6H_5CH_3$ 8·82, *189·8* (0·36)	ethanol C_2H_5OH 10·47, *188·3* (1·69)	methanol CH_3OH 10·85, *181·9* (1·70)	acetone CH_3COCH_3 9·71, *196·7* (2·88)
O_2^+ 12·07	$C_3H_7^+$(55) $C_3H_6^+$(45) 0·8 [1·6]	MH^+(45) M^+(45) $C_4H_5^+$(10) 1·5 [1·6]	MH^+ 1·4 [1·7]	M^+(75) MH^+(25) 1·2 [2·2]	$M^+(\sim 50)$ $MH^+(\sim 50)$ ~ 1 [2·3]	MH^+(60) CH_3CO^+(40) 2·8 [3·1]
NO^+ 9·26	— —	MH^+ MH^+	MH^+ —	M^+ —	$NO^+\cdot CH_3OH$ —	$NO^+\cdot CH_3COCH_3$ —
H_3O^+ 6·37	— —	MH_2^+ 1·5 [1·7]	MH_2^+ 0·7 [1·8]	MH_2^+ 0·5 [2·3]	MH_2^+ $\sim 0{\cdot}01^*$ [2·3]	MH_2^+ 1·2* [3·2]
$H_3O^+\cdot H_2O$ ~ 5	— —	MH_2^+ 2·0 [1·9]	— 2·3 [2·2]	$MH_2^+\cdot H_2O$ 2·7 [2·7]	$MH_2^+\cdot H_2O$ 2·4 [2·7]	MH_2^+(35) $MH_2^+\cdot H_2O$(65) 4·1 [3·9]
$H_3O^+\cdot(H_2O)_2$ ~ 4	— —	— 1·8 [1·6]	— —	$MH_2^+\cdot H_2O(\sim 30)$ $MH_2^+\cdot(H_2O)_2(\sim 70)$ 2·3 [2·2]	$MH_2^+\cdot H_2O(\sim 40)$ $MH_2^+\cdot(H_2O)_2(\sim 60)$ 1·9 [2·2]	$MH_2^+\cdot H_2O(> 98)$ $MH_2^+\cdot(H_2O)_2(< 2)$ 3·3 [3·1]
$H_3O^+\cdot(H_2O)_3$ $\sim 3{\cdot}5$	— —	— —	— —	— 2·1 [2·0]	— 1·9 [2·0]	$MH_2^+\cdot H_2O(> 98)$ $MH_2^+\cdot(H_2O)_2(< 2)$ 2·5 [2·8]
						2·4 [2·6]

are those of the two isomeric forms of hexenal (the known food flavour compounds trans-2-hexenal and cis-3-hexenal). The trans-2-hexenal reaction proceeds only via non-dissociative proton transfer:

$$H_3O^+ + CH_3CH_2CH_2CH{=}CHCHO \rightarrow C_6H_{11}O^+ + H_2O \qquad (4)$$

whilst there are two observed products in the cis-3-hexenal reaction:

$$H_3O^+ + CH_3CH_2CH{=}CHCH_2CHO \rightarrow C_6H_{11}O^+ + H_2O \quad (\sim 35\%) \qquad (5a)$$

$$\rightarrow C_6H_9^+ + H_2O + H_2O \quad (\sim 65\%) \qquad (5b)$$

Channel (5*a*) is the non-dissociative proton transfer channel, whereas channel (5*b*), the major channel, involves H_2O abstraction from the unsaturated aldehyde producing the linear diene ion with increased conjugation, a not uncommon reaction [10]. The reactions of both these isomers are rapid, but the rate coefficients could not be determined to the usual accuracy because of the difficulty in measuring the flow rates of the 'sticky' hexenal vapours into the flow tube. However, we estimate that they proceed at the gas kinetic rate, i.e. $k \sim k_c \sim 3 \times 10^{-9}$ cm^3 s^{-1}. The value of these observations to analysis is clear in that this ion chemistry provides a means of separately identifying these two isomers (and their quantification) when they are both present in a mixture.

2.2.2. *Reactions of OH^-*

Four of the hydrocarbons included in this study [10] (cyclohexane, cyclopropane, benzene and methylcyclohexane) do not react with OH^- ions and using the available thermochemical data [26] it is clear that there are no obvious exothermic channels in the c-C_6H_{12}, c-C_3H_6 and C_6H_6 reactions. We have no information on the thermochemistry of the negative ions derived from c-$C_6H_{11}CH_3$ so we cannot assess the ergicities of any possible reactions. That no reaction occurs between OH^- and c-$C_6H_{11}CH_3$, however, most probably means that there are no available exothermic channels in the reaction. Hence these reactions cannot be used for analysis.

The toluene reaction with OH^- has been studied previously [27] using isotopic labelling. The reaction proceeds at the gas kinetic rate generating a single ionic product:

$$OH^- + C_6H_5CH_3 \rightarrow C_6H_5CH_2^- + H_2O. \qquad (6)$$

This is a proton transfer (extraction) reaction, and the H^+ ion is extracted from the CH_3 group [27].

The results for the OH^- reaction with isoprene were somewhat surprising. The measured k for the reaction was observed to be only about $\frac{1}{3}k_c$, and three product channels were observed, two of which, according to the thermochemical data [26] are apparently endothermic:

$$OH^- + C_5H_8 \rightarrow C_5H_7^- + H_2O + 5 \text{ kcal mol}^{-1} \quad (65\%) \qquad (7a)$$

$$\rightarrow C_3H_3^- + C_2H_5OH - 10 \text{ kcal mol}^{-1} \quad (25\%) \qquad (7b)$$

$$\rightarrow C_3H_5^- + C_2H_4O - 5 \text{ kcal mol}^{-1} \quad (10\%) \qquad (7c)$$

We have discussed this surprising result and the results from a previous study of this reaction (7) in our recent paper [10]. It is sufficient to say here, because of the complexity of the reaction and the multiple products, that it is of little value in analysis.

The OH^- reactions with methanol, acetaldehyde, ethanol and acetone (which had been studied previously [27]) were observed to proceed via proton transfer at the gas kinetic rate producing only one product. According to the thermochemical data, the acetaldehyde reaction is slightly endothermic (about 0·5 kcal mol^{-1} [22]) to produce CH_3CO^-, yet we observe that $k = k_c$ for this reaction in accordance with a previous FA study [27] and so the reaction must be exothermic. This does not represent a significant problem since a small uncertainty in the heats of formation of the product negative ion is not unexpected. A previous study also showed that the proton is extracted from the CH_3 group [28].

In the reactions of OH^- with both diethyl ether and ethyl acetate two major products were observed:

$$OH^- + C_2H_5OC_2H_5 \rightarrow C_2H_5O^- \cdot H_2O + C_2H_4 \quad (60\%) \qquad (8a)$$

$$\rightarrow C_2H_5O^- + C_2H_4 + H_2O \quad (40\%) \qquad (8b)$$

It has been argued that the ionic product of channel (8*a*) is the cluster ion as indicated here because of its large binding energy [29]. The reaction of ethyl acetate proceeded thus:

$$OH^- + CH_3COOC_2H_5 \rightarrow CH_3CO_2^- + C_2H_4 + H_2O \quad (60\%) \qquad (9a)$$

$$\rightarrow {}^-CH_2COOC_2H_5 + H_2O \quad (40\%) \qquad (9b)$$

The structures of the product ions have been ascertained by previous studies [30] and are as indicated. With some care, these reactions could be used for analytical purposes.

The reactions of both the isomeric hexenals (trans-2, cis-3-hexenal) with OH^- were seen to be fast, $k \sim k_c$, and they both proceeded by proton transfer:

$$OH^- + C_6H_{10}O \rightarrow C_6H_9O^- + H_2O. \qquad (10)$$

Clearly therefore, these OH^- reactions, unlike the H_3O^+ reactions of these two hexenals, cannot be used to distinguish between the isomers. Further studies of the reactions of the isomeric forms of some other organic molecules with OH^- and H_3O^+ would be interesting and instructive.

It is worthy of note here that OH^- and its monohydrate both undergo association reactions with CO_2 and so they can be used to detect and quantify CO_2 on breath (this being of some physiological importance). The reactions proceed thus:

$$OH^- + CO_2 + M \rightarrow HCO_3^- + M \qquad (11)$$

$$OH^- \cdot (H_2O) + CO_2 + M \rightarrow HCO_3^- \cdot (H_2O) + M \qquad (12)$$

Both are three-body association reactions, the third body, M, in our laboratory experiments usually being He atoms, but in atmospheric air M would be N_2 and O_2 molecules. The three-body rate coefficients for these reactions at 300 K with the helium third body were determined in this FA study to be $k_3(14) = 5 \times 10^{-28}$ cm^6 s^{-1} and $k_3(15) = 1 \times 10^{-27}$ cm^6 s^{-1}. Whilst not fast in comparison to rapid two-body reactions at most pressures [9], these reactions are fast enough to easily quantify CO_2 on human breath because of its large partial pressure (typically a few % of the N_2).

2.3. *Reactions of* $H_3O^+ \cdot (H_2O)_{1,2,3}$ *and* $OH^- \cdot (H_2O)_{1,2}$

Hydrated hydronium ions, $H_3O^+ \cdot (H_2O)_n$, and hydrated hydroxide ions, $OH^- \cdot (H_2O)_n$, are inevitably present in ionized gases containing water, and under favourable circumstances, especially low temperatures and high pressures, the number

of clustered water molecules, n, can be very large. The binding energy of the H_2O molecule decreases with increasing n [31, 32, 33] and it is largely the reduced binding energy that limits n to 3 for the hydronium hydrates and to 2 for the hydroxide hydrates in ionised gases at 300 K. The discovery some thirty years ago of the hydronium ion hydrates in the upper terrestrial atmosphere using rocket-borne mass spectrometers [34] stimulated a great deal of interest in their formation mechanisms and their reactivity with other gases [35]. The pioneering work of Paul Kebarle and his colleagues [36] is perhaps the best source of information and understanding on the nature and reactivity of these gas phase ions. His work on ion–solvent molecule equilibria has provided most of the critical data on the binding energies of the water molecules to the core ions, and his further work on the 'switching' between the H_2O ligands and other molecular ligands has provided much of the thermochemical data on these switching processes [31, 32, 33]. The kinetics of formation of these water hydrates and of the switching rates has also received much attention [35, 37, 38], such kinetic data being necessary for the modelling of the ion chemistry of ionized media like the terrestrial atmosphere (see the references in [35]).

It should be noted that there has been a good deal of previous work on the reactions of these H_3O^+ and OH^- hydrates, references to which are given in the data compilation [9]. In our studies discussed here, some sixty reactions were involved. The reactant molecules were the hydrocarbons cyclopropane, benzene, cyclohexane, methylcyclohexane, isoprene and toluene, and the oxygen-containing organics methanol, ethanol, acetaldehyde, acetone, diethyl ether and ethyl acetate. After first describing some previous studies of the reactions of these hydrated ions, we will consider our recent studies, as before, in the following sequence: first the reactions of the positive ions with the hydrocarbons and then with the oxygen-bearing organics, followed by the reactions of the negative ions with the hydrocarbons and then the oxygen-bearing organics.

Some years ago we carried out some studies using our selected ion flow tube (SIFT) [8] of the reactions of $H_3O^+\cdot(H_2O)_{0,1,2}$ ions with D_2O and NH_3 [39] (studies to which Michael Henchman made a major contribution) and with CH_3CN [40], the results of which illustrate some of the interesting features of these cluster ion reactions. The D_2O studies revealed that in the interactions between the cluster ions and a D_2O molecule, total 'scrambling' of the H and D atoms occurs, which shows the mobility of these species in the ion–molecule transient complex. The reactions with NH_3 illustrated another common feature of these hydrated hydronium ion reactions, namely, the propensity for ligand switching and the ejection (or 'boiling off') of water molecules when the primary switching process is sufficiently exothermic, e.g.

$$H_3O^+\cdot(H_2O) + NH_3 \rightarrow NH_4^+\cdot(H_2O) + H_2O \qquad (13a)$$

$$\rightarrow NH_4^+ + 2H_2O \qquad (13b)$$

Reaction (13a) is a ligand switching reaction which is exothermic by 21 kcal mol^{-1}. We associate the positive charge with the NH_3 by virtue of its larger proton affinity ($PA(NH_3)$ = 204 kcal mol^{-1}) compared to that of H_2O (PA = 166·5 kcal mol^{-1}), a convention we adopt in all that follows. Reaction (13b) can be viewed as a proton transfer reaction, but also as a switching reaction which is sufficiently exothermic that in a fraction of the interactions the H_2O ligand (from the ion product of (13a)) is boiled off. This is energetically favourable because of the large $PA(NH_3)$; reaction (13b) is

exothermic by 4 kcal mol^{-1}. The studies with CH_3CN [40] indicated the extreme rapidity of these switching reactions when the reactant neutral has a large PA and a large dipole moment, μ_D [23]. We see several examples of these reaction processes in the new work reported in [11] which is reviewed below. These processes are considered in some detail in a very recent paper concerned with the reactions of some ethanol ion clusters [41].

2.3.1. *Reactions of $H_3O^+(H_2O)_{1,2,3}$ ions with hydrocarbons*

Of the six hydrocarbons included in the study [11], only isoprene reacts with any of the hydrated hydronium ions, and this only with the monohydrate:

$$H_3O^+(H_2O) + C_5H_8 \rightarrow C_5H_9^+ + H_2O + H_2O + 2{\cdot}4 \text{ kcal mol}^{-1}. \quad (14)$$

As can be seen, this is not a simple switching reaction but rather it should be viewed as a proton transfer reaction. The reaction is made possible by the exceptionally large PA of isoprene of 200·4 kcal mol^{-1}. It is also possible that in reaction (14) the weakly bound $C_5H_9^+ \cdot H_2O$ ions are first formed which then thermally dissociate in collisions with carrier gas atoms and so do not reach the end of the flow tube (it is interesting to note that a small signal of this cluster ion can be seen when air containing isoprene vapour is sampled into the SIFT).

It could be energetics which do not allow these protonated hydrocarbon (largely non-polar) molecules to bind an H_2O molecule and thus to inhibit switching reactions of these hydrocarbon molecules with the H_3O^+ hydrates (and the OH^- hydrates; see later). Thus, for example, from a consideration of $PA(H_2O)$, $PA(C_6H_6)$ and the H_3O^+–H_2O bond energy, it is clear that for benzene to be able to switch H_2O out of $H_3O^+ \cdot (H_2O)$, the $C_6H_7^+$–H_2O bond would need to be stronger than 17 kcal mol^{-1}. In fact, there is little evidence for the occurrence of stable hydrates of protonated aromatic and aliphatic hydrocarbons in the gas phase [9, 36] and it is unlikely that such a relatively strong bond would be formed in this system, where the proton is not localized at a particular functional group in the organic molecule. However, the hydrates of some smaller protonated hydrocarbon molecules are stable when the proton affinity of the molecule is close to that of H_2O (for example $C_2H_5^+ \cdot H_2O$, [42]). Whatever the reasons that switching reactions do not occur between $H_3O^+ \cdot (H_2O)_n$ and many hydrocarbons, this facilitates somewhat the interpretation of the complex mass spectra involved in our trace gas analysis as we will see later.

2.3.2. *Reactions of $H_3O^+ \cdot (H_2O)_{1,2,3}$ ions with oxygen-bearing organics*

Methanol, acetaldehyde, ethanol, acetone, diethyl ether and ethyl acetate were included in this SIFT study [11]. A previous FA study [43] showed that four of these molecules (namely, methanol, acetaldehyde, ethanol and acetone) undergo fast switching reactions with $H_3O^+ \cdot (H_2O)_{1,2,3}$ ions. However, this SIFT study [11] showed that the three molecules with the smaller dipole moments, μ_D, namely, diethylether, ethanol and methanol, react rapidly with $H_3O^+ \cdot (H_2O)$ and $H_3O^+ \cdot (H_2O)_2$, but they do *not* react with the $H_3O^+ \cdot (H_2O)_3$, whereas the molecules with the larger μ_D, namely ethylacetate, acetaldehyde and acetone, react rapidly with all three hydrated hydronium ions. We have no convincing explanation for the startling discrepancy between the FA and SIFT studies of the ethanol and methanol reactions with $H_3O^+ \cdot (H_2O)_3$, except to say that the SIFT is a fundamentally simpler system for such studies, and therefore less likely to produce misleading data (but see also the comments

below). The correlation of the reactivity with the μ_D of the reactant molecules is a very interesting observation, which is also helpful in the trace gas analysis work (see later in §3.2).

In the reactions of some of these oxygen-containing organic molecules with $H_3O^+\cdot(H_2O)_{1,2,3}$ ions, one or two ionic products are observed and for others no reaction is observed (table 1). The ethanol reactions exemplify all of these cases:

$$H_3O^+\cdot(H_2O) + C_2H_5OH \rightarrow C_2H_5OH_2^+\cdot(H_2O) + H_2O + 14 \text{ kcal mol}^{-1} \quad (15)$$

$$H_3O^+\cdot(H_2O)_2 + C_2H_5OH \rightarrow C_2H_5OH_2^+\cdot(H_2O)_2 + H_2O + 13 \text{ kcal mol}^{-1} \quad (70\%) \quad (16a)$$

$$\rightarrow C_2H_5OH_2^+\cdot(H_2O) + 2H_2O - 6 \text{ kcal mol}^{-1} \quad (30\%) \quad (16b)$$

$$H_3O^+\cdot(H_2O)_3 + C_2H_5OH \text{ —/→ } C_2H_5OH_2^+\cdot(H_2O)_3 + H_2O + 10 \text{ kcal mol}^{-1} \quad (17)$$

As before, we associate the proton with the molecule with the largest PA. As can be seen, reaction (15) is exothermic but not sufficiently so to disrupt the bonding of the H_2O molecule to the protonated ethanol (binding energy of 24 kcal mole^{-1} [33]). In the reactions of $H_3O^+(H_2O)$ with diethyl ether, ethyl acetate and acetone, partial 'evaporation' of the H_2O molecule does occur leaving the bare protonated organic molecule as one of the two product ions. Now in reaction (16*a*) of the dihydrate ion, switching occurs to produce the dihydrate of protonated ethanol, and apparently the monohydrate is a 30% product even though reaction (16*b*) is endothermic by 6 kcal mol^{-1} according to the available thermochemical data [22]. It is unlikely that the thermochemistry is so much in error; it is possible that the bonding of the second H_2O molecule to the $C_2H_5OH_2^+\cdot(H_2O)_2$ is weak enough that partial decomposition of the nascent molecular ion occurs (i.e. evaporation of an H_2O molecule) in its multiple collisions with the helium carrier gas atoms. As is shown above (reaction (17)) and as is mentioned at the beginning of this section, there is no reaction between the trihydrate and ethanol even though the switching reaction would be appreciably exothermic. The reason for this is probably related to the 'closed shell' nature of the $H_3O^+\cdot(H_2O)_3$ ion which inhibits the replacement of an H_2O molecule by the larger C_2H_5OH molecule. Similar steric hindrance could also explain why $H_3O^+\cdot(H_2O)_3$ ions do not react with methanol and diethyl ether [11].

As is noted above, the reactions of all the $H_3O^+\cdot(H_2O)_{1,2,3}$ ions with ethyl acetate, acetaldehyde and acetone are observed to be fast ($k = k_c$), in agreement with the previous FA observations [43]. The very large PA of ethyl acetate and acetone [22] renders these reactions sufficiently exothermic such that 'boiling off' of one or even two H_2O molecules can occur, for example:

$$H_3O^+\cdot(H_2O) + CH_3COOC_2H_5 \rightarrow C_4H_9O_2^+ + 2H_2O \quad (\sim 80\%) \quad (18a)$$

$$\rightarrow C_4H_9O_2^+\cdot(H_2O) + H_2O \quad (\sim 20\%) \quad (18b)$$

Reaction (18*a*), the 'dissociative switching channel' or the 'proton transfer channel', is only slightly exothermic (by 2·7 kcal mol^{-1}), yet it is the major channel in reaction (18). The analogous proton transfer in the acetone reaction (19*a*):

$$H_3O^+\cdot(H_2O) + CH_3COCH_3 \rightarrow C_3H_7O^+ + 2H_2O \quad (35\%) \quad (19a)$$

$$\rightarrow C_3H_7O^+\cdot(H_2O) + H_2O \quad (65\%) \quad (19b)$$

is apparently slightly endothermic (by 1·3 kcal mol^{-1}), but it also proceeds at a significant rate. However, this reaction could be thermoneutral or slightly exothermic within the accuracy of the thermochemical data, and again some thermal decomposition of the hydrate ion formed in reaction (19*b*) could be occurring along the flow tube of the SIFT, thus increasing the observed $C_3H_7O^+$ fraction. In the trihydrate ion reactions with acetaldehyde, ethyl acetate and acetone, up to two H_2O molecules are 'boiled off':

$$H_3O^+\cdot(H_2O)_3 + CH_3COCH_3 \rightarrow C_3H_7O^+\cdot(H_2O) + 3H_2O \quad (>98\%) \qquad (20a)$$

$$\rightarrow C_3H_7O^+\cdot 2H_2O + 2H_2O \quad (<2\%) \qquad (20b)$$

Clearly, these hydrated hydronium ions have value in trace gas analysis in that their reactivity can be exploited to distinguish between polar and non-polar molecules. We will demonstrate this in our discussions of trace gas analysis in §§3 and 4.

2.3.3. *Reactions of $OH^-(H_2O)_{1,2}$ ions with the hydrocarbons*

In the light of previous work, it is not surprising that no switching reactions were observed between the OH^- hydrates and the weakly-polar hydrocarbons included in this study [11]. Electron transfer from the ions to these hydrocarbons is endothermic by virtue of the relatively large electron affinity of the OH radical (1·83 eV [26]) and the relatively large binding energies of the H_2O ligands [32]. These FA studies clearly showed that OH^- hydrates only react at a measurable rate with polar molecules as is discussed in the following section.

2.3.4. *Reactions of $OH^-\cdot(H_2O)_{1,2}$ ions with the oxygen-bearing organics*

Diethyl ether does not react with either of these OH^- hydrates; significantly this ether has a relatively small μ_D of 1·15 D [23]. Ethanol undergoes fast switching reactions with both the hydrates generating the ethoxide water clusters:

$$OH^-\cdot(H_2O) + C_2H_5OH \rightarrow C_2H_5O^-\cdot(H_2O) + H_2O \qquad (21)$$

$$OH^-\cdot(H_2O)_2 + C_2H_5OH \rightarrow C_2H_5O^-\cdot(H_2O)_2 + H_2O \qquad (22)$$

In both of these reactions, only one H_2O molecule is ejected, this probably being determined by the available energy (reaction (10) is exothermic by only 10 kcal mol^{-1}). The two corresponding methanol reactions are also fast, and in one of them, the dihydrate reaction, two products are observed:

$$OH^-\cdot(H_2O)_2 + CH_3OH \rightarrow CH_3O^-\cdot(H_2O) + 2H_2O \quad (\sim 60\%) \qquad (23a)$$

$$\rightarrow CH_3O^-\cdot(H_2O)_2 + H_2O \quad (\sim 40\%) \qquad (23b)$$

and reaction (23*a*) is sufficiently energetic to eject two H_2O molecules from the intermediate complex. Again, the production of $CH_3O^-\cdot(H_2O)$ could be partly due to the thermal decomposition of $CH_3O^-\cdot(H_2O)_2$ in the flow tube.

In each of the reactions of the remaining three molecules in this group, ethyl acetate, acetaldehyde and acetone, an obvious reduction is observed in the k with increasing hydration of the OH^- ion, to the extent that there is no measurable reaction between $OH^-\cdot(H_2O)_2$ and ethyl acetate and acetone. The k for the reaction of $OH^-\cdot(H_2O)_2$ with acetaldehyde is only $\sim 20\%$ of k_c, but both H_2O molecules are retained in the product cluster ion:

$$OH^-\cdot(H_2O)_2 + CH_3CHO \rightarrow C_2H_3O^-\cdot(H_2O)_2 + H_2O \qquad (24)$$

Used alone, the hydrated hydride ions have limited value in analysis, but used together with OH^-, and especially with H_3O^+ and its hydrates, they can indicate which of the trace gases have appreciable μ_D.

2.4. *Reactions of NO^+ and O_2^+*

Much is known about the ion chemistry of these two ions in atmospheric air [35, 44]. They are the primary ions in the terrestrial stratosphere and mesosphere which undergo slow termolecular reactions with the abundant ambient molecules (N_2, O_2, H_2O, CO_2) [9, 45], reactions which are essential steps in the synthesis of the observed terminating $H_3O^+(H_2O)_n$ ions in these atmospheric regions [35]. However, as mentioned in the Introduction, the important point with respect to trace gas analysis is that NO^+ and O_2^+ do not undergo bimolecular reactions with the major air constituents at significant rates, and so they are potentially useful as precursor ions in the analysis of air. Some studies of the bimolecular reactions of NO^+ and O_2^+ have been carried out [9, 46], but there have been no systematic studies of the reactions of these ions with a variety of organic molecules of relevance to trace gas analysis of air and human breath. It is known that NO^+ and O_2^+ ions undergo charge transfer reactions with some organic molecules with low ionization potentials (such as CH_3NH_2 [46] and some other molecules [9]), and that NO^+ reacts with some molecules by H^- transfer [9, 47], but the data base is sparse. Hence we carried out a SIFT study of the reactions of these ions in their ground vibronic states with 10 organic species, the hydrocarbons benzene, toluene, isoprene, cyclopropane and *n*-pentane, and the oxygen-containing organics, methanol, ethanol, acetaldehyde, acetone and diethyl ether. The detailed results of this study which are reported in our recent paper [12] are now summarized.

2.4.1. *The NO^+ reactions*

The attraction of NO^+ ions as precursors in the trace gas analysis of air is their low recombination energy (9·25 eV) which ensures that these ions cannot ionize the major air components which have high ionization potentials (IP). Hence only molecules with IP less than 9·25 eV can be ionized in charge transfer collisions with ground state NO^+ ions to produce their parent ions. There are three reactions in the above series in which this process occurs, these being the toluene, benzene and isoprene reactions. In all three reactions non-dissociative charge transfer occurs, exemplified by the benzene reaction:

$$NO^+ + C_6H_6 \rightarrow C_6H_6^+ + NO \tag{25}$$

According to the published values, the IP of NO and benzene are very close, reaction (25) being barely exothermic. This may explain why the measured rate coefficients, k, for this charge transfer reaction is $\frac{2}{3}k_c$, the k for the toluene reaction is $\frac{1}{2}k_c$, and that for the isoprene reaction is equal to k_c. It is worthy of note that the k for charge transfer reactions are often less than k_c, because the efficiencies of such reactions are reduced by such parameters as unfavourable Franck–Condon factors and steric hindrance [48, 49]. This contrasts with the k for proton transfer reactions which, when exothermic, are always equal to k_c at thermal energies [17], as is indicated in the previous §§2.2 and 2.3.

The IP of the remainder of the reactant molecules included in this study exceed that of NO and so charge transfer between vibronic ground state NO^+ and these molecules cannot occur at thermal energies. However, other reaction processes do occur, these being hydride ion (H^-) transfer and association reactions. Thus the diethyl ether,

acetaldehyde and ethanol reactions each proceed by H^- transfer producing the appropriate ion and neutral HNO radicals (not H atoms) as demanded by the energetics of the reaction (thermochemical data taken from [22]). In the reaction:

$$NO^+ + C_2H_5OH \rightarrow CH_3CHOH^+ + HNO \qquad (26)$$

the energetics require that not only is HNO produced but also that the structure of the product ion is as indicated (protonated acetaldehyde), and is not the other stable structural isomer $C_2H_5O^+$. This reaction is relatively inefficient, the measured k being only about $\frac{1}{4}k_c$ (table 1) in accordance with the results of a previous study [47]. The analogous H^- transfer reaction with CH_3CHO is similarly inefficient, but the similar $C_2H_5OC_2H_5$ reaction proceeds at a rate close to the collisional rate (see [12] for details).

Bimolecular reactions do not occur at measurable rates between NO^+ and acetone, methanol, cyclopropane and *n*-pentane. At first sight it is curious why H^- transfer occurs in the ethanol reaction (26) whereas it does not occur in the methanol reaction:

$$NO^+ + CH_3OH \not\rightarrow CH_2OH^+ + HNO \qquad (27)$$

The answer is simple; reaction (26) is exothermic by 16 kcal mol^{-1} whereas reaction (27) is endothermic by 5 kcal mol^{-1}. (Note that the production of the CH_3O^+ isomer in reaction (27) would be much more endothermic.) However, termolecular association is observed in the methanol and the acetone reactions, e.g.

$$NO^+ + CH_3COCH_3 + He \rightarrow NO^+ \cdot CH_3COCH_3 + He \qquad (28)$$

Here, the stabilizing 'third body' is a helium atom which carries away the binding energy of the cluster ion. This reaction is very efficient at the temperature (300 K) and pressure (0·5 Torr) of the helium carrier gas in these SIFT measurements, the measured (effective) bimolecular rate coefficient being about $\frac{1}{3}k_c$ for the initial NO^+/CH_3COCH_3 collisions (table 1). This is equivalent to a very large termolecular association rate coefficient of $> 5 \times 10^{-26}$ cm^6 s^{-1}.

There is some evidence in the published literature that NO^+ ions react at quite different rates with the different structural isomers of some hydrocarbons. For example, apparently the reaction of NO^+ with iso-butane is very fast, whereas its reaction with *n*-butane is immeasurably slow [50]. So we looked at the reactions of NO^+ with trans-2-hexenal and cis-3-hexenal. The reactions proceeded efficiently thus:

$$NO^+ + CH_3CH_2CH_2CH{=}CHCHO \rightarrow C_6H_9O^+ + HNO \qquad (29)$$

$$NO^+ + CH_3CH_2CH{=}CHCH_2CHO \rightarrow C_6H_9O^+ + HNO \quad (60\%) \quad (30a)$$

$$\rightarrow C_4H_6O^+ + (C_2H_3 + NO) \quad (25\%) \quad (30b)$$

$$\rightarrow C_4H_5O^+ + (C_2H_4 + NO) \quad (15\%) \quad (30c)$$

Reaction (29) apparently proceeds via the relatively simple process of H^- transfer, whereas reaction (30) is more complex resulting in three products.

Comments are made later on the analytical value of these data for the NO^+ reactions and also the data for the O_2^+ reactions which are now discussed.

2.4.2. *The O_2^+ reactions*

The recombination energy of O_2^+ (12·06 eV) is almost 3 eV greater than that of NO^+ and so charge transfer is energetically possible in the reactions of O_2^+ with all the molecules included in this limited survey. All these reactions are fast, and dissociative charge transfer is possible in some reactions and is indeed observed. In the benzene and

toluene reactions, the only products are the parent ions $C_6H_6^+$ and $C_7H_8^+$, again indicating the stability of the aromatic rings, and both reactions are fast, i.e. $k \sim k_c$. However, in the reactions of the two aliphatic hydrocarbons isoprene and *n*-pentane, dissociative charge transfer channels are observed, e.g.

$$O_2^+ + CH_2{=}C(CH_3)CH{=}CH_2 \rightarrow C_5H_8^+ + O_2 \quad (45\%) \quad (31a)$$

$$\rightarrow C_5H_7^+ + (H + O_2) \quad (45\%) \quad (31b)$$

$$\rightarrow C_4H_5^+ + (CH_3 + O_2) \quad (10\%) \quad (31c)$$

The uncertainty in the energetics of these reactions is such that we cannot be sure if the radicals HO_2 and CH_3O_2 have to be formed in channels (31*b*) and (31*c*); hence the use of the brackets around the neutral products. In the *n*-pentane reaction two product ions are observed:

$$O_2^+ + \text{n-}C_5H_{12} \rightarrow C_3H_6^+ + C_2H_6 \quad (45\%) \quad (32a)$$

$$\rightarrow C_3H_7^+ + C_2H_5 \quad (55\%) \quad (32b)$$

These reaction channels are sufficiently exothermic that both the open-chain and the cyclic isomers of the product ions could be formed [22], as is also the case for the cyclopropane reaction in which the two observed products are $C_3H_6^+$ (90%) and $C_3H_5^+$ (10%). Both reaction (32) and the cyclopropane reaction are fast with the k being close to k_c for both reactions.

A common feature of the reactions of O_2^+ with the oxygen-containing organic molecules, MH, included in this study is the occurrence of both non-dissociative and dissociative charge transfer products. Thus the parent ion MH^+ is always formed in some proportion and a common product is also M^+ ions which result from the elimination of an H atom from the excited MH^+. Both processes are very obvious in the acetaldehyde, ethanol and methanol reactions as, for example,

$$O_2^+ + C_2H_5OH \rightarrow C_2H_4OH^+ + H + O_2 \quad (30\%) \quad (33a)$$

$$\rightarrow C_2H_5OH^+ + O_2 \quad (70\%) \quad (33b)$$

These dissociative charge transfer reactions are sufficiently exothermic that the HO_2 radical need not be formed (although HO_2 is a well-known stable radical implicated in tropospheric chemistry [51]). The methanol reaction proceeds in a similar way producing CH_3OH^+ ($\sim$ 50%) and CH_2OH^+ ($\sim$ 50%) [46], as does the acetaldehyde reaction producing CH_3CHO^+ (55%) and CH_3CO^+ (45%) [12]. The k for these reactions are: CH_3CHO, k_c; C_2H_5OH, $\frac{1}{2}k_c$; CH_3OH, $\frac{1}{2}k_c$.

The acetone reaction proceeds thus:

$$O_2^+ + CH_3COCH_3 \rightarrow CH_3COCH_3^+ + O_2 \quad (60\%) \quad (34a)$$

$$\rightarrow CH_3CO^+ + CH_3 + O_2 \quad (40\%) \quad (34b)$$

In this reaction the very stable ion CH_3CO^+ is formed. The diethyl ether reaction is also largely dissociative charge transfer producing $C_3H_7O^+$ as the major product (80%) and $C_4H_{10}O^+$ and $C_4H_9O^+$ as minor products. Both these reactions are fast with the k being appreciable fractions of their k_c.

2.5. *Potential of H_3O^+, OH^- and their hydrates, NO^+ and O_2^+ for trace gas analysis*

It is clear from this survey that H_3O^+ ions are very reactive with a wide range of hydrocarbons and many other organic molecules, the k for their proton transfer reactions being closely equal to the respective k_c when the PA of the reactant molecule

exceeds that of H_2O. This renders H_3O^+ ions superb chemical ionization agents for trace gas analysis as we and others have shown [3, 10, 52]. OH^- ions are also reactive with many organic compounds, but the k and the products of the reactions are not so predictable [9] and so their use in quantitative analysis is not so straightforward.

An important point to emphasize at the onset of this discussion is that when many ions, and certainly H_3O^+ and OH^-, are introduced into 'wet' air such as room air and especially human breath, then clustering of the ions to the abundant water molecules occurs. This clustering is especially efficient for H_3O^+ ions whence the hydrated hydronium ions are formed. Then reactions of the trace gases in the air (or the air sample introduced into the SIFT) may occur with both the precursor ion, H_3O^+, and the H_3O^+ $(H_2O)_{1,2,3}$ ions. This complicates the product spectrum and makes its interpretation and the quantitative analysis of the trace gases more challenging. These hydrated H_3O^+ ions (and also the OH^- hydrates) have some analytical value in that it is now clear that non-polar molecules (e.g. hydrocarbons) generally do not react with these hydrates whereas the polar molecules do. So by observing whether or not switching reactions occur can be an indication of the nature of the reactant molecule.

Both NO^+ and O_2^+ ions cluster much more slowly to H_2O molecules than do H_3O^+ ions, and so we observe that when the former ions are injected into the carrier gas in the SIFT apparatus configured for trace gas analysis, then whilst cluster ions of the type $NO^+(H_2O)_m$ and $O_2^+(H_2O)_n$ are indeed observed, they are a small fraction of the precursor ion count rates at the detection mass spectrometer (see §§2.1 and 3.2). This alleviates a complication in the trace gas analysis and it is thus a positive aspect of the use of NO^+ and O_2^+ precursor ions.

An undisirable aspect of the reactions of NO^+ ions in analysis is the wide variety of processes that occur (charge transfer, hydride-ion transfer and termolecular association reactions) and the variability of the rate coefficients, k, which are often significantly smaller than k_c. This contrasts with the simpler exothermic proton transfer reactions of H_3O^+ ions. However, one valuable use we have found for NO^+ precursor ions is in the positive identification and quantification of isoprene and methanol on human breath [12]. When H_3O^+ ions are used for this purpose, a complication arises in that the mass of protonated isoprene, $C_5H_9^+$, coincides with the mass of the dihydrated protonated methanol ion $CH_3OH_2^+(H_2O)_2$, both at 69 u. This complicates the separation and the accurate analysis of these trace gases. Fortunately, however, NO^+ does not react with methanol at a significant rate whereas it reacts at the collisional rate with isoprene to produce a single product (table 1), and so this provides an unambiguous method for distinguishing between methanol and isoprene on breath. So we conclude in general that NO^+ ions have limited value in analysis, except that they can be used for the accurate quantification of particular trace gases, and that they can provide useful information when used together with H_3O^+.

The reactions of O_2^+ with organic molecules are charge transfer reactions producing the parent organic ion or dissociative charge transfer reactions resulting in two or three fragments of the parent ion. The greater recombination energy of O_2^+ ions ensures that they usually react rapidly with most molecules including, significantly, many that do not react with H_3O^+ ions such as the lower order aliphatic hydrocarbons [9]. This then is the real value of O_2^+ in trace gas analysis. We have found it useful as a detector of *n*-pentane which does not react with H_3O^+ and which is present on human breath (being an indicator of free radical activity in the body [53]). However, O_2^+ precursor ions must be used with some circumspection, because often more than one ion product results, as indeed is the case in its reaction with n-pentane (reaction (32)

and table 1). O_2^+ also reacts with both NO and NO_2 [9], both present in polluted air [51]. We have recently detected NO on human breath at the 100 ppb level (as expected [54]) using our SIFT approach and O_2^+ as the precursor ions [55]. Further, O_2^+ reacts rapidly with CS_2 (another breath compound [56]) whereas H_3O^+ only reacts slowly with this molecule because of its low proton affinity [42]. So the value of O_2^+ in trace gas analysis is clear. We find that the use of H_3O^+ and O_2^+ together has particular value, an approach we are now beginning to use routinely in our SIFT trace gas analysis work.

3. Application of the SIFT to trace gas analysis

3.1. *Preliminary comments on conventional analytical mass spectrometry*

We have already noted in § 1 that the analysis of atmospheric air or breath sampled via a controlled leak into the low pressure electron impact ion source of a conventional mass spectrometer has severe limitations. The required operating pressure of a mass spectrometer (magnetic sector and quadrupole) is typically 10^{-5} Torr and below, and the leak from atmosphere must not allow the pressure to increase above this approximate value. Thus the partial pressure of a trace gas in the ion source present at say 1 ppm in the atmosphere cannot be greater than about 10^{-11} Torr. The combined effects of this low partial pressure, the low efficiencies for ionization of low pressure electron impact ion sources, and the inevitable fragmentation of organic molecules under electron impact (cracking), result in very low ion currents and therefore very poor detection sensitivity and when several trace gases are present, many ion peaks appear in the mass spectrum. Also fragment ions of the same mass-to-charge ratio often result from the cracking of different molecules. The spectrum is then very difficult to interpret. So air and breath analysis by direct air sampling into conventional mass spectrometers has been limited to components present at percentage or fractional percentage levels, and with a lower limit of about 100 ppm.

3.2. *Chemical ionization using the SIFT*

An answer to the above problems is to sample the atmosphere (or breath) at higher flow rates into the ion source (the ionizer or the reactor), and to use softer ionization (no cracking), i.e. chemical ionization. These conditions can be met using the SIFT (and FA) method. This is best illustrated by way of an example; here we choose the detection of acetone (CH_3COCH_3) in air utilizing H_3O^+ precursor ions and thus exploiting the reaction:

$$H_3O^+ + CH_3COCH_3 \rightarrow H_2O + CH_3COCH_3 \cdot H^+. \tag{35}$$

This proton transfer reaction occurs with unit efficiency (table 1) and, very significantly, without any molecular fragmentation, i.e. only the protonated acetone molecule is formed and so mass spectrometric identification is relatively easy.

So in our SIFT experiment configured for air analysis, H_3O^+ ions are generated in the remote ion source as described in §2.1, and after mass selection they are injected into the carrier gas when they are convected along the flow tube and detected by the downstream mass spectrometer/ion counting system (figure 1). Count rates up to the limiting value for a channeltron are possible ($\sim 10^6$ s^{-1}). Now the air or breath (with the trace of acetone) is introduced into the carrier gas at a suitable (measured) flow rate and reaction (35) occurs. The count rate of the H_3O^+ at the detector in the presence of the acetone, n, is related to the count rate in the absence of acetone, n_0, by the equation:

$$n = n_0 \exp -k[A]t \tag{36}$$

where $[A]$ is the number density of the acetone in the flow tube (i.e. in the carrier gas), k is the rate coefficient for reaction (35) and t is the reaction time defined as the ratio of the distance, z, between the air (and acetone) sample entry port and the downstream mass spectrometer sampling orifice (figure 1) and the flow velocity, v, of the ion swarm, i.e. $t = z/v$. The parameters k, v and z are readily measured [8] and so from a determination of n and n_0, a value for $[A]$ can be obtained. For low values of $[A]$ the count rate of protonated acetone ions is simply equal to $n_0 k[A]t$, i.e. directly proportional to $[A]$.

A typical flow rate of *carrier gas* in the SIFT is 100 atm cm^3 s^{-1} (6 standard litres per minute) [8] which establishes a carrier gas number density of about 10^{16} cm^{-3} in the flow tube, and so the air sample can be introduced at a few percent of this without seriously disturbing the flow. At a partial pressure of about 1 ppm of acetone in the air, such a flow rate of the air establishes an acetone number density in the carrier gas, $[A]$, of about 10^9 cm^{-3}. Given that the k for reaction (35) is $3{\cdot}9 \times 10^{-9}$ cm^3 s^{-1} (table 1 and [9, 10]) and that t is typically a few milliseconds in our SIFT experiment, then the product $k[A]t$ is $\sim 10^{-2}$. So the count rate of protonated acetone ions is about 1 % of the H_3O^+ count rate. Clearly, even for a modest count rate of H_3O^+ of 10^5 per second, the $CH_3COCH_3 \cdot H^+$ count rate is $\sim 10^3$ per second which is readily detected with very good statistics. For higher H_3O^+ count rates the detection sensitivity is increased proportionally. This then is the basic principle of the SIFT detection and analysis technique. The FA technique [13] is essentially identical except that there is no upstream mass selection of the primary reactant ion. Rather a microwave gas discharge through the carrier gas is used, the advantage of this being that much larger primary ion count rates are realized at the downstream mass spectrometer with the corresponding increase in the detection sensitivity. However, the price that is paid for this is that the primary ion swarm is not 'pure' (as it is in the SIFT) but rather a mixture of ions, and so one must be very careful not to misinterpret minor downstream mass spectrometer signals which can arise from ionic reactions involving primary ions other than H_3O^+.

As was previously discussed, H_3O^+ reacts with the H_2O in the air (breath) sample primarily to regenerate H_3O^+ (symmetrical proton transfer) and to form 'clusters', i.e.

$$H_3O^+ + nH_2O + M \rightarrow H_3O^+ \cdot (H_2O)_n + M. \qquad (37)$$

These are examples of three-body association reactions, the rates of which are increased by high pressures, i.e. by high number densities of the 'third body' M. These hydrated hydronium ions also react with the trace acetone in ligand switching reactions such as reactions (15), (16) and (20) producing the monohydrate and dihydrate of protonated acetone (table 1) and in our trace gas analysis these reactions are similarly exploited as an additional detection and diagnostic tool, using the kinetic data on the switching reactions obtained from the SIFT studies [11, 39, 45].

H_3O^+ ions (or the hydrates) do not react with the major atmospheric constituents N_2, O_2, Ar and CO_2 (which all have relatively low proton affinities). But all the trace gas species, A, with proton affinities greater than that of water will be protonated by the H_3O^+ ions and so AH^+ ions appear on the mass spectrum at count rates directly proportional to the concentrations of A in the air sample (actually, weighted by the rate coefficients, k, for their reactions with the H_3O^+ ions [57]). Product ions from the reactions of the water cluster ions will also appear and these must be analysed in the same way and the concentration of A in the sample calculated accordingly. The

required k are obtained from the compilations of data and other papers [8, 9, 10, 11], much provided from SIFT studies of the kind discussed above, or in the case of the proton transfer reactions the k ($=k_c$) are readily calculated using ion–molecule rate theory [18]. Because the product ions generally do not undergo cracking, multi-component mixtures can be analysed quantitatively. So the value of this technique for detecting trace gases in air is clear. The fact that only polar trace gases (e.g. acetone) undergo switching reactions with the water cluster ions [11] helps in the identification of some trace gases. So, for example, when there is more than one candidate trace gas species at a given mass-to-charge ratio, then whether or not switching patterns are observed gives a very important clue as to the nature of the molecule (see the case of CH_3CN in §4.4).

The principle of operation of this SIFT analytical technique is identical whatever precursor ion is used, but of course the appropriate (measured) k for the reactions involved must be used. As is indicated above, the k for charge transfer reactions (e.g. the O_2^+ reactions) are often smaller than their respective k_c, and so these k must be taken from the literature. If they are not available, they can be measured using the SIFT technique.

4. Some initial results of the trace gas analysis of breath

It has been known since the last century that certain gases on human breath are indicators of adverse clinical conditions, e.g. the presence of excess acetone (originally detected by the smell) being an indicator of diabetes [58]. More recent research work has applied modern techniques to the detection and quantification of trace gases on breath, including gas chromatography of samples collected in bags made from suitable materials, and breath sampled directly into a device that removes most of the water from the sample before the remaining trace gases are trapped and concentrated onto some form of breath trap (cryogenic and adsorption traps have been used) and then released into a gas chromatograph and assayed using mass spectrometry [59]. Using these techniques a large number of gases (perhaps 400) have been detected on the breath of healthy persons at concentrations within the partial pressure range of about 1 to 1000 ppb (parts per billion) [56]. However, these methods of breath sampling and quantification have obvious drawbacks; the sampling into bags involves the potential danger of selective condensation of the trace gases on the bag surface, and the efficiency of adsorption may vary with the nature of the trace gases.

Clearly a device is required that can be used to simultaneously analyse several trace gases in breath, down to the ppb regime in real time, preferably from a single exhalation and with a fast time response. Ideally, the device should also be portable. With such a device the screening of the breath of people in different environments such as hospitals, doctor's surgeries, factories and domestic environments, as well as the monitoring of patients in the congested space of intensive care units could be carried out. This is a major motivation for the development of our selected ion flow tube (SIFT) [8] and the flowing afterglow (FA) [13] techniques (and hybrids of these) for trace gas analysis. In this section of the paper we present some examples of our first results of breath analysis which illustrate the enormous potential of our method.

4.1. *The analysis of trace gases in the helium carrier gas of the SIFT, in the laboratory air, and on the breath of a healthy, non-smoking individual*

4.1.1. *The helium carrier gas*

It is, of course, important to establish at the onset the levels of detectable impurities in the SIFT carrier gas (helium in these experiments). This is simply achieved by injecting the H_3O^+ ions and recording the mass spectrum at the downstream mass spectrometer. A typical result is shown in figure 2(*a*), where the mass spectrometer count rates are shown on a log scale to illustrate the count rate range and sensitivity available. The scan covers 100 u and was taken for a period of 120 seconds, i.e. a dwell time of 1·2 s per mass unit. The 'background' count rate is less than one count in 10 s, and so one count per second (c s^{-1}) is a lower limit to a meaningful measurement, and this sets the ultimate sensitivity of the apparatus. For a count rate of the precursor H_3O^+ ions of 10^5 c s^{-1}, a k of 10^{-9} cm^3 s^{-1} for the proton transfer reaction involving a molecular X producing XH^+ ions, and a reaction of time of 5×10^{-3} s, then one c s^{-1} of the product ions XH^+ is equivalent to 10^6 molecules per cm^3 in the helium. At a He number density of 2×10^{16} cm^{-3}, one c s^{-1} is equivalent to 50 parts per trillion (ppt) of X in the helium! However, as has been stated several times, the major atmospheric species N_2, O_2 and H_2O, do not react with H_3O^+, and it is these which are expected to be the major impurities in the helium. So H_3O^+ precursor ions will not detect these impurity species. But as can be seen in figure 2(*a*), the major impurity ions on the spectrum are indeed derived from N_2 (N^+, N_2^+ and N_2H^+ the last ionic species resulting from the reaction of N_2^+ with the impurity H_2O), O_2 (O^+ but mostly O_2^+), and H_2O (OH^+ and H_2O^+). The $H_3O^+ \cdot (H_2O)$ cluster ions are formed in the three-body association reactions between the H_3O^+ (reaction (37)) ions and the water impurity in the helium (at a partial pressure of a few ppm). The H_2O impurity can be reduced by scrubbing the helium with a cold trap, but in practice this is not necessary because a much larger amount of water is introduced in the air sample to be analysed.

So what is the origin of these 'air ions'? The answer comes from the observation that there are also ions in the spectrum at a mass-to-charge ratio of 20 u and 40 u, these being Ar^{++} and Ar^+ ions. The Ar^{++} ions are formed by the double ionization of argon atoms in the argon/water ion source gas and a small fraction is injected into the carrier gas together with the H_3O^+ ions (19 u) at a current of about 1 % of the H_3O^+ current. These energetic ions react at the gas kinetic rate by single charge transfer with N_2, O_2 and H_2O [9] producing the observed atomic and molecular impurity ions and Ar^+ ions. It can be shown using the simple analysis outlined in §3.2 that a total partial pressure of only about 1 ppm of N_2 and O_2 in the helium is required to give the level of impurity ions shown in figure 2(*a*). (In our more recent experiments we have been able to completely remove Ar^{++} from the injected ion beam by better filtering in the injection mass filter.) It should also be noted that the O_2^+ ions are formed partially by the photoionization of the impurity O_2 by the UV radiation that penetrates into the carrier gas from the microwave discharge ion source. This phenomenon is more obvious when air is introduced into the carrier gas for analysis (figures 2(*b*) and 2(*c*)).

4.1.2. *Laboratory air*

Figure 2(*b*) shows the mass spectrum after the introduction into the helium of laboratory air at a flow rate of 1 torr litre s^{-1}, i.e. 1 % of the helium flow rate, which we used in all the measurements that are reported below. As can be seen, the major new ions on the spectrum are the water cluster ions $H_3O^+ \cdot (H_2O)_{2,3}$ formed by the sequential association reactions of the precursor H_3O^+ ions with the H_2O in the air

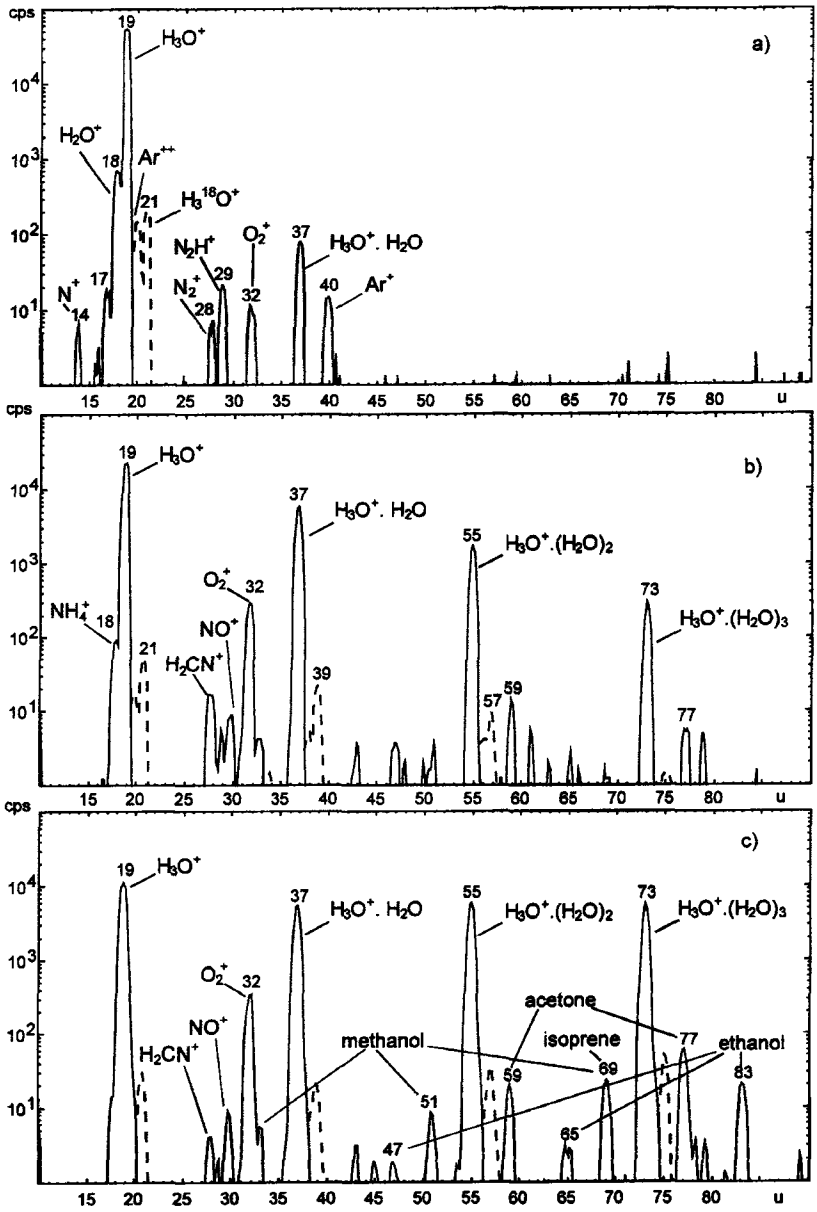

Figure 2. (*a*) The ion spectrum observed by the downstream mass spectrometer of the SIFT following the injection of H_3O^+ into cylinder helium carrier gas at a pressure of 0·5 Torr in the flow tube. Note that the signal levels vary over four to five orders of magnitude. Minor signals S(< 1 %) of N^+, OH^+ (17 u), H_2O^+ and Ar^{++} (at 20 u) are also transmitted by the quadrupole mass filter. The other ions seen on this spectrum are largely the result of the reactions of these injected ions with air impurities in the helium and subsequent ion–molecule reactions. The $H_3O^+ \cdot H_2O$ ions are formed in the three-body reaction between the H_3O^+ ions and water impurity in the helium. Note the appearance of the $H_3{}^{18}O^+$ isotopic ion (dashed) at mass 21 u. (*b*) The modified spectrum of (*a*) following the introduction of a small flow (1 Torr l s^{-1}) of laboratory air into the helium carrier gas. Note the appearance of the water cluster ions $H_3O^+ \cdot (H_2O)_{1,2,3}$ and their associated ^{18}O isotopic variants (dashed). Note also the NH_4^+, H_2CN^+ and the ions at 59 and 77 u derived respectively from traces of NH_3, HCN and acetone in the laboratory air, and the now

sample, together with the associated ions two mass units higher in each case, these being the ^{18}O isotopic variants at signal levels in accordance with the naturally-occurring $^{16}O/^{18}O$ isotope ratio of about 500:1. Note, however, that these cluster ions represent about 20% of the total ion count rate. Note also that most of the 'impurity ions' (with the notable exception of O_2^+) which are present in the spectrum in figure 2(*a*) are not present. This is because all the ions derived from Ar^{++}, including Ar^+, react with the large amount of N_2 and O_2 introduced into the carrier gas largely producing the terminating (relatively unreactive) ions O_2^+ and a little NO^+ (hence the reason why these last ions are potentially useful precursor ions in the trace gas analysis of air!). Photoionization (see above) is also partly responsible for the relatively large signal of O_2^+. The other minor ions on the spectrum are indicative of the trace gases in the laboratory atmospheric air. The ions resulting from the presence of acetone are immediately recognisable; that at 59 u is protonated acetone and that at 77 u is the monohydrate of protonated acetone. From these data the acetone is calculated to be present at the 100 ppb level in this laboratory air. The ions at 18 u and 28 u are NH_4^+ and H_2CN^+ formed from traces of NH_3 and HCN in the laboratory air (the mass 28 u ions cannot be either N_2^+ or CO^+ because these ions are very reactive with both O_2 and H_2O). The value of this analytical technique to environmental monitoring is immediately clear, a facility which we will be exploiting very much in the future.

4.1.3. *Human breath*

Figure 2(*c*) shows the spectrum obtained when human breath is introduced into the carrier gas at our standard flow rate. This sample of breath from a healthy, non-smoking person was taken from a sample bag which had first been purged with clean artificial air before it was filled by the individual. This method of breath sampling allows spectral scans to be accumulated over longer periods (in this case again 120 s), although the danger is that condensation of some trace gases from the same can occur onto the bag surface (this can be minimized by holding the bag surface just above body temperature). Alternatively, a breath sample can be introduced into the apparatus by simply blowing through an open tube connected to the entrance pipe (figure 1), which allows the mass spectrum to be obtained of a single exhalation of breath (over a maximum time of about 10 s) as we show in the next section. First notice in figure 2(*c*) that the water cluster ions represent a greater fraction of the total signal than they do for the sample of laboratory air (figure 2(*b*)); this is because the breath sample is much wetter. Then, as before, there are peaks at 59 u and 77 u which are protonated acetone ($CH_3COCH_3 \cdot H^+$) and its monohydrate respectively. The peaks at 33 u, 51 u and 69 u are identified as protonated methanol ($CH_3OH_2^+$) and its mono- and dihydrate respectively, the last two ionic species being formed principally in switching reactions of the water cluster ions with the trace methanol in the breath sample. The 69 u peak we also attribute partly to protonated isoprene ($CH_2C(CH_3)CHCH_2 \cdot H^+$). This coincidence of the masses of protonated isoprene and the protonated methanol

larger signal of relatively unreactive O_2^+ ions which are additionally formed by photoionization of the O_2 in the introduced air sample by energetic photons from the discharge ion source. (*c*) The modified spectrum of (*a*) following the introduction of a breath sample from a healthy person (again at a flow rate of 1 Torr l s^{-1}). Note the increase in the signal levels of the water cluster ions because of the greater humidity of breath compared to laboratory air. Note also the increase in the signal level of the acetone-derived ions, and the appearance of ions derived from isoprene, ethanol and methanol (see text for further explanation and also figure 4).

dihydrate was discussed in §2.5. We will show in §4.2 another very interesting manifestation of this mass coincidence when we consider the time-resolved signals of the isoprene and methanol on a single exhalation of breath. As is mentioned in §2.3, non-polar and weakly polar gases, including isoprene, do not undergo these switching reactions and so there is only one peak on the spectrum for isoprene derived from its reactions with both the H_3O^+ and $H_3O^+ \cdot H_2O$ ions [10, 11] and there are no hydrated protonated isoprene ions. Also seen on the spectrum are ions at 65 u and 83 u, these being the mono- and dihydrates of protonated ethanol. The partial pressure of these gases on the breath can be obtained using the sums of all the product ion count rates on the spectrum associated with each individual neutral trace gas species, ratioed to the sum of all the precursor $H_3O^+ \cdot (H_2O)_n$ ions weighted by the rate coefficients; the details of this analysis are given in a recent paper [57]. Our limited survey of several individuals in the laboratory indicates that the partial pressure of acetone on the breath of a healthy individual is typically within the limited partial pressure range of 0·5 to 2 ppm, but we find the isoprene to be more variable, usually within the range 0·1 to 1 ppm. Isoprene is known to be the most abundant hydrocarbon on breath [60], and a high level of this gas on breath has been associated with mental stress [56]. Examples of these partial pressures are given in the next section. Note that the signal levels of the O_2^+ and NO^+ ions are very similar in both the spectra of the air and the wetter air shown in figures 2(*b*) and 2(*c*), this again being an indication that these ions are not very reactive with water. However, the 28 u peak (H_2CN^+ ions) is obviously smaller in figure 2(*c*) indicating that these ions are more reactive with water.

4.2. *A demonstration of the rapid time response of the SIFT analytical system using breath acetone and isoprene as the indicators*

The time response of this SIFT system is largely determined by the flow times of gases along the sampling tube and the flow tube. Currently, it is only about 20 ms. We are thus able to see the trace gas exhalation profiles as a person displaces the laboratory air with breath at the entrance to the sampling port. This can be done either by an ambient air inhalation/exhalation breath cycle which thus introduces into the flow tube the 'background' gases on the inhalation cycle, or by breathing clean cylinder air via a one-way (Rubin) valve from the cylinder equipped with a breathing bag as used in anaesthetic breathing circuits (figure 1). This results in very low 'background' ion count rate at all masses. Then we can programme the on-line computer system to tune the detection mass spectrometer either to fix on a particular ionic mass or to switch rapidly between several different masses, and then record different ion count rates during the breathing cycle. An example of the breathing cycle as followed using the protonated acetone hydrate, $CH_3COCH_3 \cdot H^+ \cdot H_2O$, at mass 77 u is shown in figure 3(*a*). The variations between the breath profiles are almost entirely due to the variations in the flow of breath from the individual. The four cycles are overlapped in the inset of the figure to illustrate the consistency of these breath concentration profiles. In this example the mean value of the acetone partial pressure on the breath, accounting for all the acetone-containing ions on the mass spectrum, is close to 1·5 ppm. Shown in figure 3(*b*) are the breath profiles obtained simultaneously for the acetone (again using the ion at 77 u) and for the trace gases which produce the ions at 69 u. Note the obvious structure on the profile of the 69 u ion. We now understand that this is due to the coincidence of the masses of protonated isoprene and the dihydrate of protonated methanol as referred to in §§2.5 and 4.1. This structure is a common feature of the breath profile at the 69 u ions, and we tentatively explain it

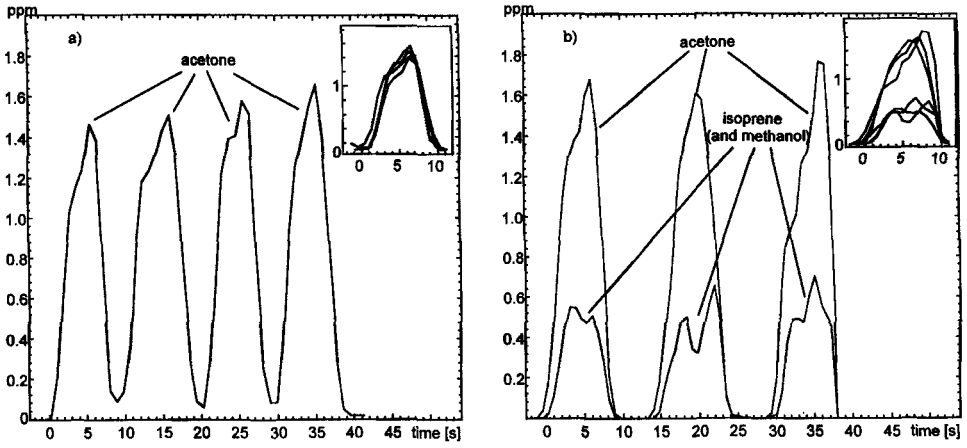

Figure 3. (*a*) Time profiles of breath acetone concentration (in ppm, of the breath gas) from a subject breathing with a cycle of about once per ten seconds directly into the SIFT apparatus. The precursor ions are H_3O^+ and its hydrates. These profiles were obtained by rapidly switching the SIFT mass spectrometer between the primary and product ions. The absolute partial pressure of the acetone on the breath is then calculated from the count rates of the acetone product ions (at 59 u and 77 u) and those of the primary (precursor) ions (at 19 u, 37 u, 55 u and 73 u) by the procedure outlined in §3.2 (and given in more detail in [57]) using the known rate coefficients for the proton transfer and switching reactions. The four breath cycles are overlapped in the inset to the diagram to show the consistency of these cycles. Note the initial rapid rise in the amount of acetone exhaled during the first two seconds as the upper airways are emptied and then the slower further increase as the alveolar breath is exhaled. The fluctuations on each profile are real indicators of the acetone flow fluctuations, because the time constant of the system is only about 20 ms. (*b*) Breath profiles of both the acetone and isoprene obtained simultaneously by the rapid switching of the SIFT mass spectrometer between ions derived from the acetone (in this case 59 u and 77 u), an ion derived from both isoprene and methanol (69 u) and the primary ions. We tentatively suggest that the peculiar structure on these profiles is due to the differing flow rates of isoprene and methanol from the lungs (see text). The three breath samples are again overlapped in the inset to the diagram.

by a difference in the rate of outflow of isoprene and methanol from the lungs (perhaps the result of the different solubilities of these compounds in the mucous lining of the bronchial tract?). This idea can be checked by minimizing the proportions of $H_3O^+(H_2O)_{1,2,3}$ ions (the important source of the protonated methanol hydrates) relative to H_3O^+ ions (the major source of the protonated isoprene), this being achieved by reducing the flow of wet breath into the SIFT. Alternatively, NO^+ precursor ions could be used to differentiate between isoprene and methanol (see the previous discussion in §2.5). We estimate that the isoprene concentration on this breath sample is several times lower than that of the acetone, as is usually the case. However, this is not always so, and the isoprene on the breath of apparently healthy individuals is much more variable than the acetone concentration ([61]). One of the many objectives of our research is to monitor the isoprene on the breath of selected individuals over the daily cycle and over periods of weeks.

4.3. *Time variations of breath vapours after the ingestion of a significant quantity of ethanol*

It is obvious that our novel technique for breath analysis can also be utilized to follow the time decay of gases on breath over very long as well as very short time

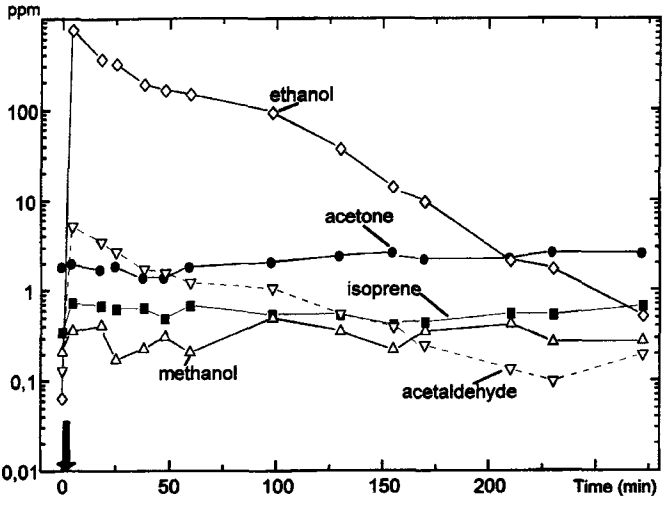

Figure 4. Decay curves of the concentrations (in ppm) of five substances on the breath of an individual following the ingestion of distilled liquor. The precursor ions were H_3O^+ and its hydrates. All five concentrations at each time are the mean concentrations in a *single* exhalation of breath. Note that the large increase in the ethanol concentration is accompanied by an increase in the acetaldehyde concentration, and that the acetone, isoprene and methanol levels do not change much during the whole observational period of nearly five hours.

intervals. We have recorded the breath of a colleague over a period of several hours following the consumption of 150 ml of distilled liquor, a rather large drink! Several gases were recorded simultaneously in intervals of 10 to 50 min from a *single exhalation* as described above, and the end-expiratory concentrations are shown in figure 4. The ethanol quickly appears on the breath at a high concentration near to 800 ppm, rather too high for our detector which tends to become non-linear at these high partial pressures. (To accurately quantify vapour at this very high partial pressure, a sampling flow rate at least 10 times smaller would be necessary.) Initially, the ethanol concentration on the breath decreases linearly with time (see also [61]), but at concentrations lower than about 100 ppm the ethanol decays exponentially with time, the time constant for the loss of ethanol on the breath of this individual being about 30 minutes. Acetaldehyde also appears on the breath at a much lower level, and it apparently decays more slowly with a time constant of about one hour, reaching the pre-drinking level after about four hours. However, acetaldehyde is apparently formed by the metabolism of ethanol and so the observed decay rate is a combination of its formation and loss rates. Note that a low concentration of methanol was present on this individual's breath before drinking the ethanol and that the concentration did not change significantly with the ingestion of the large amount of ethanol. Note also that the inevitable breath acetone and isoprene concentrations also remain sensibly constant during the four hour observational period, indicating that the biochemistries that produce these compounds are not apparently influenced by the presence in the blood stream of a good deal of ethanol.

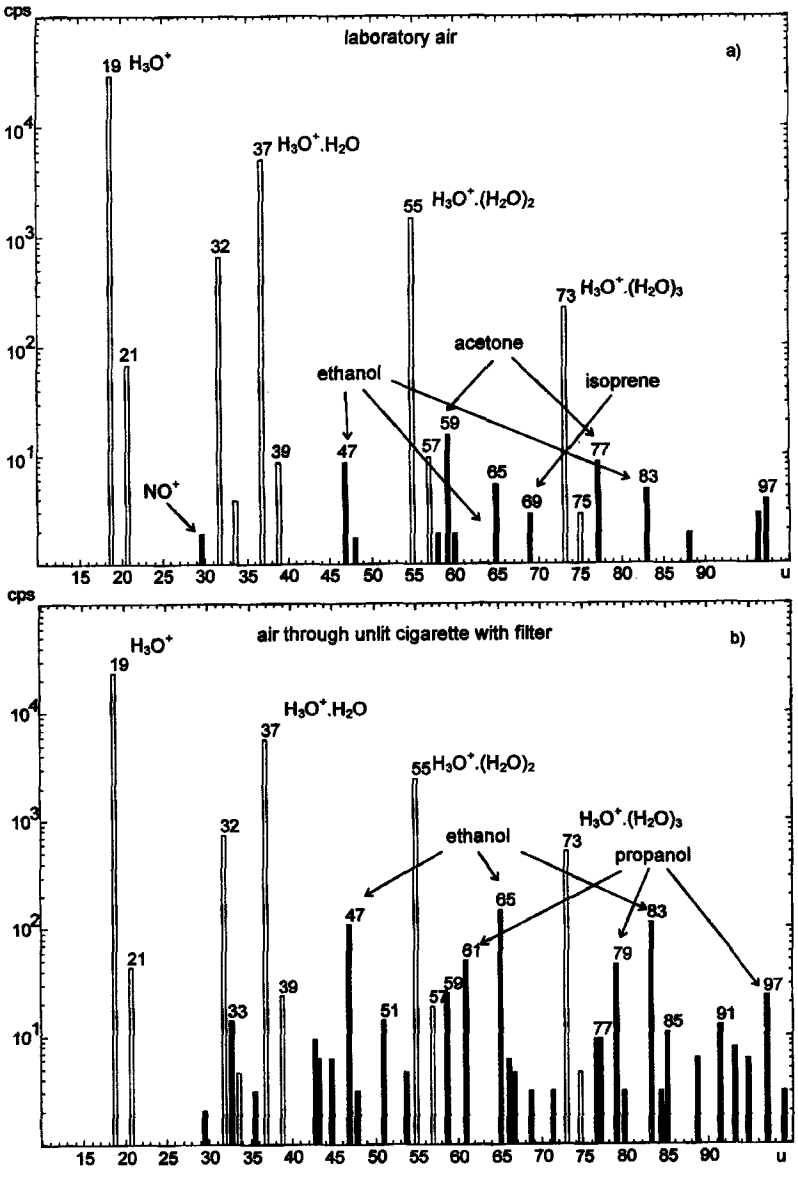

Figure 5. (*a*) The spectrum is the SIFT following the introduction of the laboratory air, given here as a standard. The open bars are the $H_3O^+ \cdot (H_2O)_n$ 'primary' ions with their ^{18}O isotopic variants and the (unwanted) O_2^+ ions, and the black bars are the ions indicating the trace gases in the laboratory air on that occasion. (*b*) The spectrum obtained when the laboratory air is drawn through an unlit cigarette with a filter directly attached to the input port of the SIFT. Note the appearance of the ions of protonated ethanol and its hydrates at masses 47 u, 65 u and 83 u and similarly those most probably derived from either propanol, acetic acid or methyl ethyl ether (or a mixture of these) at masses 61 u, 79 u and 97 u. Other ions at much lower levels are also present which we have not attempted to identify at this stage.

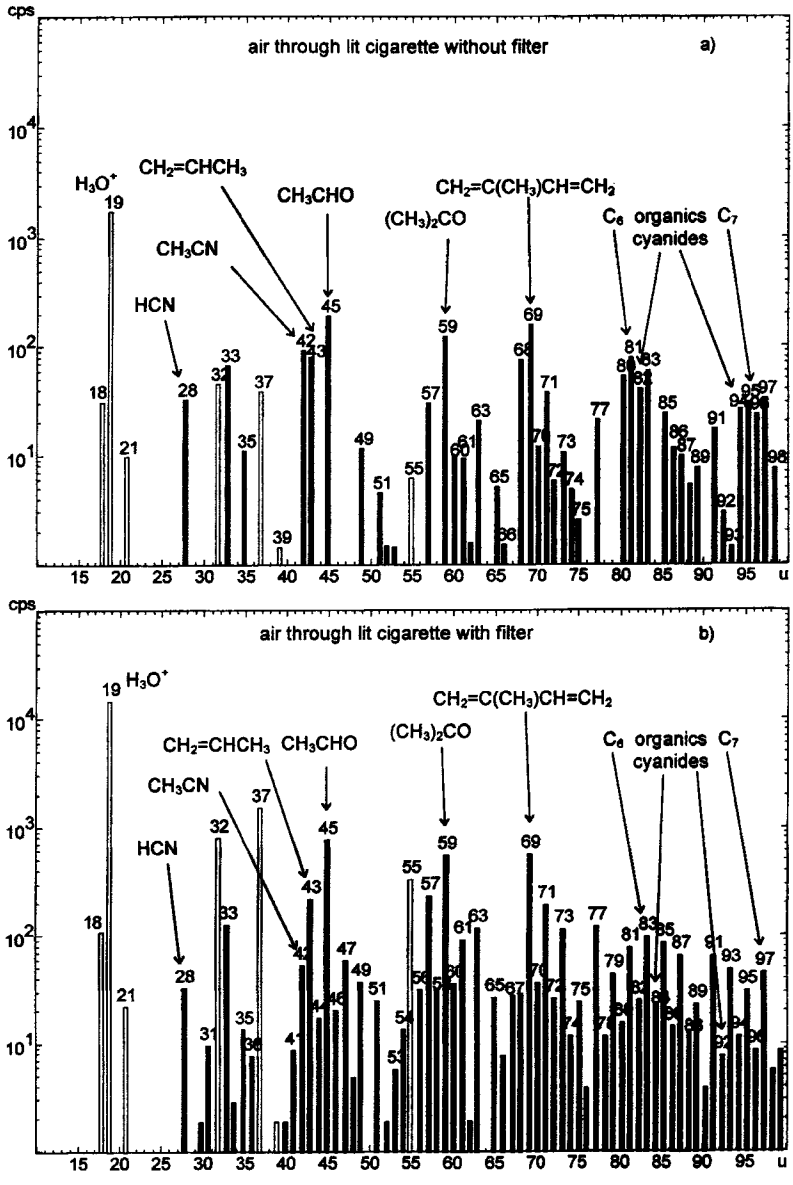

Figure 6. (*a*) The spectrum obtained when the cigarette used to obtain the data of figure 5(*b*) but with the filter removed is lit. Again the open bars are the 'primary' ions. An amazing array of ions appears on the spectrum which we attribute to the presence in the cigarette smoke of hydrocarbons, aldehydes, ketones and cyanides some of which we identify on the figure. Present are HCN, CH_3CN and CH_2=$CHCH_3$ (shown in figure 7(*b*)), which are retained on the breath of a smoker. Note also that the signal level of the precursor ion H_3O^+ is considerably lowered when the cigarette is lit (compare with figure 5(*b*)). This is an indication of the very large number of molecules that are in the smoke that react with H_3O^+, and also demonstrates that there are many more ionic species formed at very large masses that are not recorded by this limited-scan (100 u) mass spectrum (we see ions with masses up to the current limit of our mass spectrometer of 400 u). (*b*) The mass spectrum obtained with the lit cigarette but with the filter included. Note that the overall signal levels are obviously greater, immediately indicating that some of the reactive molecules

4.4. *A comparison of the mass spectra obtained for laboratory air, cigarette smoke and for the breath of a non-smoker and a smoker*

To best illustrate the results of these preliminary studies, we present a series of spectra in histogram form obtained for laboratory air (§4.4.1) and laboratory air drawn through an unlit cigarette (§4.4.2), then air drawn through a lit cigarette without the filter (§4.4.3) and air drawn through the same brand of a lit cigarette with the filter (§4.4.4), and finally the breath of a non-smoker (§4.4.5) and the breath of a smoker (§4.4.6). We limit the mass spectral range to 100 u to avoid complication. A comment will be made later concerning ions of greater mass.

4.4.1. *The sample of laboratory air*

The spectrum obtained of the sample of laboratory air is shown in figure 5(*a*). As can be seen, it is relatively simple and very like the spectrum shown in figure 2(*b*) which is also for the air in the same laboratory and of which a full interpretation is given in §4.1.2. It is interesting to note that the signal levels of the ethanol and acetone in this air are each equivalent to a partial pressure of about 50 ppb). This then is the starting condition for the subsequent analyses.

4.4.2. *The unlit cigarette*

Figure 5(*b*) shows the spectrum obtained when the laboratory air is drawn through the unlit cigarette. The new peaks observed are in two series, these being 47 u, 65 u and 83 u, and 61 u, 79 u and 97 u. Notice that the difference in the masses between these two series is 14 u, which is indicative of a CH_2 group (note that this cannot be due to a nitrogen atom because the neutral (unprotonated) molecules are of even mass). Thus two different compounds are involved with molecular weights of 46 u and 60 u together with their mono- and dihydrates. The possible identities of these compounds are ethanol (C_2H_5OH) and either n- or iso-propanol (C_3H_7OH) because of the sweet-smelling nature of the unlit cigarette, although dimethyl ether (CH_3OCH_3) and perhaps formic acid (HCOOH) for the former, and methyl ethyl ether ($CH_3OC_2H_5$) and perhaps acetic acid (CH_3COOH) for the latter cannot be ruled out. (Note that the intensities of the ^{13}C variants of these ions could be used to distinguish between the C_1, C_2 and the C_3 species when this is necessary.) These compounds are present in this air sample drawn through the unlit cigarette at a total level of about 1 to 2 ppm; only the cigarette manufacturer knows why they are present! There is also a small signal at mass 59 u which is most probably protonated acetone. Note that the monohydrate of this ion at 77 u is present. Other ions at much lower signal intensities (< 10 c s^{-1}) are also present which are, as yet, unidentified.

4.4.3. *A lit cigarette without the filter*

Figure 6(*a*) shows the horrendous spectrum obtained for a lit cigarette with the filter removed (smoked directly into the SIFT). The first point that must be made is that the air drawn through the lit cigarette is obviously much drier than the laboratory air and so, as can be seen, the $H_3O^+ \cdot (H_2O)_{1,2,3}$ ions are at much lower levels relative to H_3O^+. The second important point is that the intensity of the primary H_3O^+ ions is much smaller in the absence of the filter (figure 6(*b*)), which is a clear indication that

are removed from the smoke and so do not enter the flow tube. Presumably, some of the very large molecules (the tar) are removed by the filter and it is apparent that the lower order cyanides are somewhat more efficiently removed than are the aldehydes, but many more measurements need to be made to substantiate these observations.

much more reactive material is entering the flow tube, this in turn indicating that there are molecules of very high molecular weight in the smoke, many of which are removed by the filter when it is present. We identify here some of the most obvious compounds that are present, noting again that the spectrum shows the protonated molecules and so the neutral molecules are of molecular weight one mass unit less than the detected ions. Thus some of the neutral species present (in brackets) are as follows:

18 (ammonia, NH_3);
28 (hydrogen cyanide, HCN);
31 (formaldehyde, H_2CO with its mono and dihydrate ions at 49 u and 67 u);
33 (methanol, CH_3OH, with its monohydrate ion at 51 u);
42 (acetonitrile, CH_3CN and its monohydrate on at 60 u);
43 (propene, $CH_2{=}CHCH_3$); $C_3H_7^+$ (from propanol);
57 (acrolein (propenal), $CH_2{=}CHCHO$);
59 (acetone, CH_3COCH_3, or propanal, CH_3CH_2CHO, or allyl alcohol, $CH_2{=}CHCH_2OH$ with the monohydrate ion at 77 u);
61 (n- or iso-propanol (C_3H_7OH), methyl ethyl ether ($CH_3OC_2H_5$), or acetic acid (CH_3COOH) with the monohydrate ion at 79 u);
68 (C_4H_5N, allyl cyanide, $CH_2{=}CHCH_2CN$, or butenonitrile, $CH_3CH{=}CHCN$, or methacrylonitrile, $CH_2{=}C(CH_3)CN$) or even pyrrole, C_4H_4NH);
69 (isoprene, $CH_2C(CH_3)CHCH_2$, or butynal, $CH_3C{\equiv}CCHO$, or furan, C_4H_4O with a component of the dihydrate of protonated methanol);
71 (C_5H_{10}, pentene isomers);
a group of ions around mass 80 (probably including C_6 hydrocarbons e.g. benzene);
a group of ions around mass 94 (probably including C_7 hydrocarbons).

The ions at masses 59 u, 61 u, 68 u and 69 u may well be due to more than one of the species indicated. The unambiguous identifications are of NH_3, HCN, H_2CO, CH_3OH, CH_3CN, $CH_2{=}CHCH_3$ and $CH_2{=}CHCHO$. Some doubt remains concerning the identification of the other compounds, although it is certain that isoprene (seen previously [56, 59]) is a component of mass 69 (§4.2), and that unsaturated cyanides and aldehydes are also formed in the burning tobacco. The indicated higher-order hydrocarbons are also present, and mass scans up to 200 u indicate the presence also of C_8 hydrocarbons and other species of higher molecular weight. We intend to combine gas chromatography with our SIFT method to positively identify more of these compounds.

4.4.4. *A lit cigarette with the filter*

The spectrum obtained for the same brand of lit cigarette with its filter attached is shown in figure 6(*b*). A comparison of this with figure 6(*a*) shows that the filter apparently absorbs a fraction of the nitrogen-bearing organics such as HCN, CH_3CN, and the neutral species with masses 67, 79 and 81 u, but apparently not so well the aldehydes and the hydrocarbons. Also, as mentioned above, the very large molecules ('tar') are partially removed by the filter. Therefore many different gases enter the mouth and lungs of the smoker.

4.4.5. *The breath of a non-smoker*

Figure 7(*a*) shows a typical spectrum obtained from the breath of a non-smoker. As can be seen, there are minor ions due to protonated methanol and its hydrates (33 u, 51 u and a fraction of the signal at 69 u), protonated ethanol and its hydrates (47 u, 65 u, 83 u), larger signals due to protonated acetone and its monohydrate (59 u,

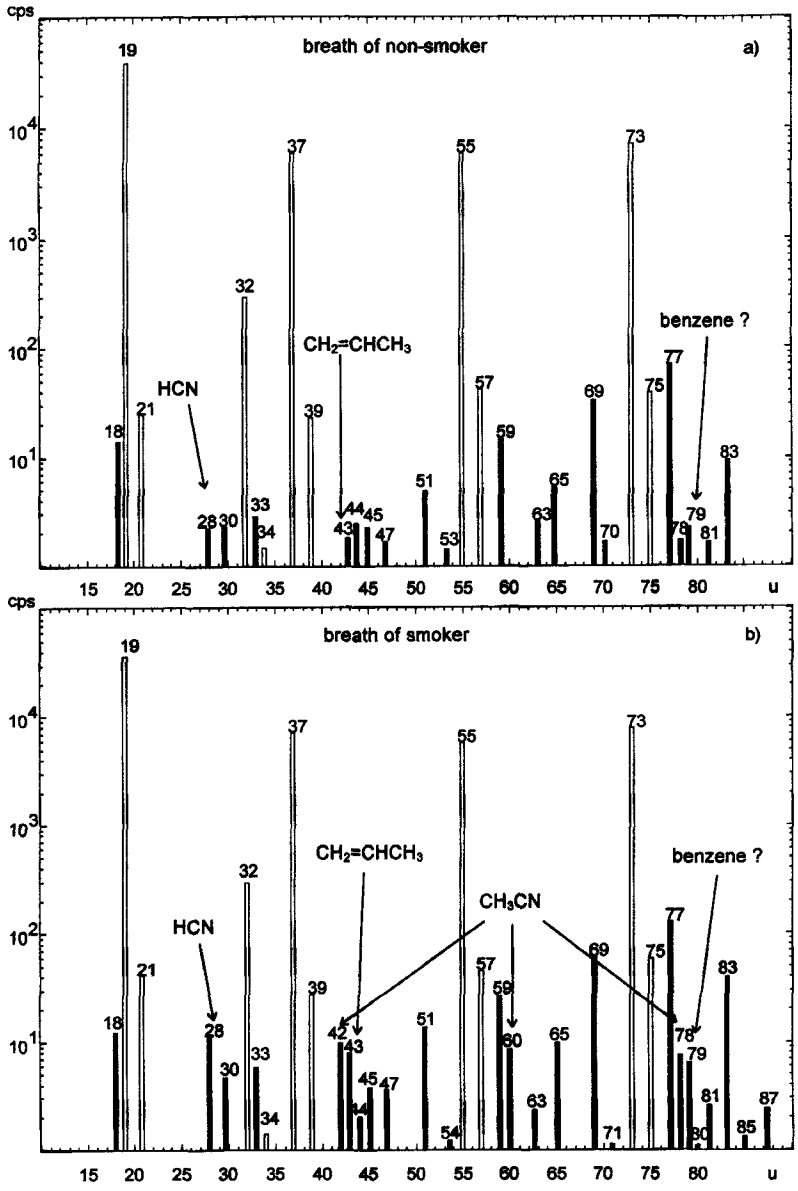

Figure 7. (*a*) The spectrum of the breath of a non-smoker (H_3O^+ and its hydrates as precursors) clearly showing as before (figure 2(*c*)) the acetone (59 u and 77 u), isoprene (69 u), ethanol (47 u, 65 u and 83 u), methanol (33 u and 51 u) and traces of acetaldehyde-related peaks (45 u, 63 u and 81 u). Small signals are present due to HCN, CH_2=$CHCH_3$ (propene) and possibly benzene (but see text). Again the much larger open bars are the 'primary' ions. (*b*) The spectrum of the breath of a smoker. The most obvious additional ions (compared to the non-smoker's breath) are at 42 u, 60 u and 78 u which are $CH_3CN \cdot H^+$ (protonated acetonitrile) and its first and second hydrates. Note that the protonated HCN and CH_2=$CHCH_3$ and the mass 79 u ion are much more obvious, and these together with the acetonitrile ions are potential markers of a smoker's breath. The larger ethanol-derived peaks (at 47 u, 65 u and 83 u) are also clear. (Note, however, that HCN is apparently present at a low level in the laboratory air also; see figure 2(*b*).)

77 u), and protonated isoprene (a fraction of the signal at 69 u; note again that this protonated non-polar hydrocarbon does not form a hydrate [11]) As has been mentioned previously, both acetone and isoprene are present on the breath of all healthy human beings [56, 59, 61]. Minor signals at 28 u (H_2CN^+), 30 u (NO^+; see the discussion in §4.1), and 79 u (possibly protonated benzene) are also seen. However, other ions appear on the spectrum of a smoker's breath.

4.4.6. *The breath of a smoker*

Figure 7(*b*) shows the spectrum obtained for the smoker's breath 30 min after smoking a cigarette, and it can be seen immediately that additional ions are present, and some of those seen in figure 7(*a*) are much more obvious. The peak at 28 u is much bigger, and is indicative that HCN, present in cigarette smoke, is retained on the smoker's breath. Similarly, the ion at 43 u is more intense, and this we attribute to the presence of propene on the smoker's breath (very obvious on the spectrum of the cigarette smoke (figure 6(*a*)). The peak at 79 u is larger which could be indicative of protonated benzene or protonated fumaronitrile ($CNCH{=}CHCNH^+$) or even protonated dimethylsulphoxide ($(CH_3)_2SOH^+$). The most obvious additional ion occurs at 42 u which must be protonated acetonitrile, CH_3CNH^+. Protonated acetonitrile is known from our previous studies [40] to readily form hydrates, and so it is no surprise to see its hydrates appear on this spectrum at masses 60 u and 78 u. It is also clear that the ions due to ethanol are more intense than on the non-smoker's breath; clearly, this subject had been drinking as well as smoking! The acetone and isoprene concentrations are not so different than those for the non-smoker's breath, and are certainly within the likely natural variations of these compounds in breath. But it is clear that HCN, CH_3CN and $CH_2{=}CHCH_3$ persist on the breath of smokers, and so they are good indicators that an individual has been smoking. Other molecules are present at a level < 10 ppb as is indicated by the ions at 54 u, 71 u and 87 u. Clearly, an enormous amount of interesting and valuable research can be done in following up these very preliminary studies.

5. Other applications of the SIFT analytical technique

5.1. *Analysis of vapours emitted by foods and food flavours*

Our preliminary contacts with the food processing industry have revealed to us the importance of determining the composition of the vapours (odours) emitted by foods and food products in order to assess their 'freshness' and also to assist in the creation of attractive odours. (Also, there is obviously a great deal of interest in the development of personal products such as toothpaste and deodorants in which trace gas analysis is important.) Thus, as a first entry to this interesting and commercially important topic, we have used our SIFT method to look at the complex mixtures of vapours emitted by some fruits, mostly as an indicator of the value of our technique in this challenging area.

5.1.1. *The vapours emitted by a banana*

A very graphic example of the power of the technique is seen in the sensing of the vapours emitted by a ripe banana. Thus we simply hold a peeled banana near the entry port of the SIFT as it continually samples the laboratory air, again using H_3O^+ precursor ions in the analysis. The resultant spectra shown in figure 8 is quite amazing!

First consider figure 8(*a*) which is a mass scan up to 110 u, where many familiar ions are present including protonated methanol and its hydrates (33 u, 51 u, 69 u) and

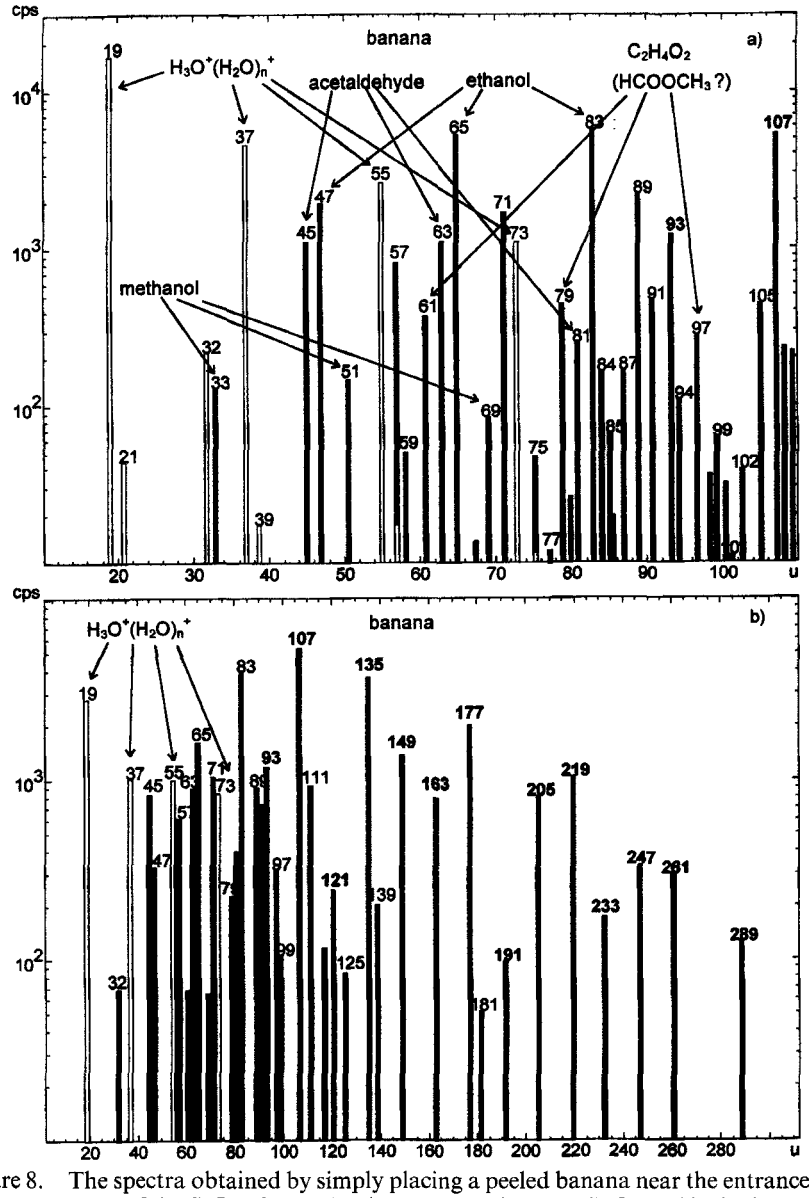

Figure 8. The spectra obtained by simply placing a peeled banana near the entrance to the gas entry port of the SIFT (figure 1). The precursor ions are H_3O^+ and its hydrates as shown. (*a*) The low mass scan up to 110 u showing the presence in the banana vapour of methanol, ethanol, acetaldehyde and a polar species with molecular weight of 60 u and molecular formula $C_2H_4O_2$ which could be $HCOOCH_3$ (but see text). Some other unidentified molecules are also present at lower levels. (*b*) The spectrum scanned up to 300 u showing many larger mass ions which apparently fall into an homologous series (differing by 14 u) labelled with bold numbers. We discuss the possible origin of these ions in the text. The monohydrates of some of these ions are also obvious (e.g. at 111 u, 139 u).

similarly ethanol (47 u, 65 u, 83 u), acetaldehyde (45 u, 63 u, 81 u) and ions at 61 u, 79 u and 97 u which could be either protonated acetic acid or methyl formate and their hydrates. Note that the largest signals from these particular compounds are from the ethanol component. There is also a significant signal at masses 71 u, 89 u and 107 u,

again indicating a core protonated molecule of mass 70 u and its hydrates. The most likely molecular formula of this neutral molecule is C_4H_6O (remembering that it has a large dipole moment because it switches with water hydrates; so it is not a hydrocarbon). There are then several possibilities for this species including methacrolein (CH_2=(CH_3)CHO), butenal (CH_3CH=CHO) and divinyl ether ((CH_2=CH)$_2$O). The obvious signal at 57 u has only a low intensity hydrate at 75 u, and so we judge that it is largely due to a protonated hydrocarbon with molecular formula C_4H_8, being most probably a butene (which unlike butane have proton affinities greater than that of H_2O). The alternative polar molecule would be acrolein. (Note that there is an overlap between these ions and the ^{18}O variants of the $H_3O^+(H_2O)_{2,3}$ ions.)

But now consider the wider mass scan shown in figure 8(*b*). It is apparent that the ions in the spectrum above 100 u form an homologous series, their masses differing by 14 u and therefore differing by a $-CH_2$ group. Actually, this series apparently begins at 93 u (and perhaps even 79) and progresses at 107 u, 121 u, 135 u, 149 u, 163 u, 177 u, 191 u, 205 u, 219 u, 233 u, 247 u, 261 u, missing 275 u, and then 289 u. This is a remarkable 14 (or 15) molecular species! The monohydrates of 93 u (111 u), 107 u (125 u), 121 u (139 u) and 163 u (181 u) can also be seen, but interestingly they are not present for the larger mass ions. This last observation suggests that all 14 ions may not form a single homologous series; perhaps the second 7 species are an homologous series of hydrocarbons? But what is the lowest mass neutral species at 92 u? Isotopic analysis indicates that the molecular formula is $C_3H_8O_3$, whence glycerol is a possibility.

It is possible that fewer than 14 different molecular species are present in this banana vapour, since if the proton affinities of those molecules that are present are very large then when they accept the proton from H_3O^+, dissociation of the ion could occur possibly producing multiple fragment ions which could form homologous series in CH_2 (see reactions (38) and (39) below). Gas chromatography could be of help in deciding which of these species are involved. Of course, it is possible that more than one of these species is present on the banana vapour, which in any event is quite a cocktail! The important point to emphasise is that conventional mass spectrometry would be of little value in the analysis of such a complex mixture, whereas using this SIFT/chemical ionization technique much can be learned about the composition of complex gas mixtures.

5.1.2. *The vapours emitted by an onion*

We have also looked at the vapours emitted from a sliced uncooked onion, and the spectra obtained are shown in figure 9. The low mass spectrum is not very complex; at low masses protonated methanol, acetaldehyde and ethanol and their hydrates are evident again (especially obvious are the ethanol-derived ions), but also very obvious are the ions at masses 77 u (and the hydrate at 95 u) and 91 u (say XH^+) and its hydrate at 119 u ($XH^+(H_2O)$) which is a relatively large signal because the onion vapour is very wet. Also very obvious is the ion at 181 u which we believe to be the proton-bound dimer of the species at 90 u, XH^+X (such proton-bound dimers of polar molecules, including, of course, $H_3O^+(H_2O)$, are very well-known; see Michael Henchman's superb paper [62]). Isotopic analysis of the 109 u ion is shown in an inset to figure 9, where the ^{13}C and ^{34}S isotopes of carbon and sulphur are very obvious. Careful measurement of the abundances of these isotopes reveals that the molecular formula of the included polar molecule of mass 90 u is $C_4H_{10}S$. Inspection of the lists of organic

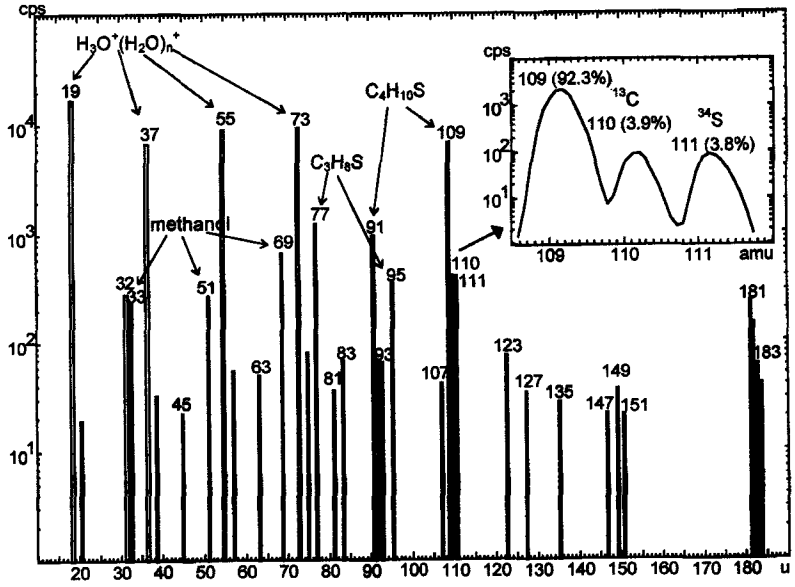

Figure 9. The spectrum obtained by placing a peeled onion near the gas entry port of the SIFT. The precursor ions are H_3O^+ and its hydrates as shown. The ions at 77 u and 91 u are due to the onion vapour (with their monohydrates at 95 u and 109 u respectively). The black bars indicate the ^{13}C and ^{34}S variants of the larger hydrate signals of these ions, and the inset to this figure shows the higher resolution spectrum of these isotopic variants of the 109 u ion. From these isotopic signal levels it is clear that the ion comprises four carbon atoms and one sulphur atom, and hence the likely molecular formula of the neutral organic molecule at mass 90 u is $C_4H_{10}S$. Possible identifications of this molecule are given in the text. Also obvious on the spectrum is the proton-bound dimer of this molecule at 181 u, $C_4H_{10}SH^+C_4H_{10}S$ (together with the isotopic variants). Some other minor ions are present in the 123 u to 151 u mass range.

compounds with this molecular formula in the *CRC Handbook* [23] indicates that there are at least ten structural isomers that are possible, including several thiols (mercaptans), RSH, and alkyl sulphides, R_1SR_2. Then the ion at 77 u, probably possessing a CH_2 group less than the 91 u, is C_3H_8S. Thus, for example, these molecules may be methyl ethyl sulphide, $CH_3SC_2H_5$, and diethyl sulphide, $(C_2H_5)_2S$. Further we cannot say, except that continuing these examples, the ion at 181 u would be $(C_2H_5)_2SH^+S(C_2H_5)_2$. Again, gas chromatography allied to this SIFT method would be a very valuable approach to the analysis of these vapours.

5.1.3. *The food flavours*

As an extension to these studies, we have looked at some specific compounds used as food flavours and toothpaste additives. Again using H_3O^+ precursor ions, we accumulated the product mass spectra for the following compounds (listed in pairs, the reason for which will become clear) which were kindly supplied to us by the UNILEVER Colworth Research Laboratory in the UK. (i) 2-hexenal (98 u) and 2-methyl pyrazine (94 u); (ii) n-hexanal (100 u) and 3-hexenal (98 u); (iii) menthone (154 u) and limonene (136 u). The ion spectra thus obtained for these compounds are shown in the montage in figure 10.

The spectra for the first pair of compounds (i) show that only the protonated parent molecules (99 u and 95 u respectively) are produced in the primary proton

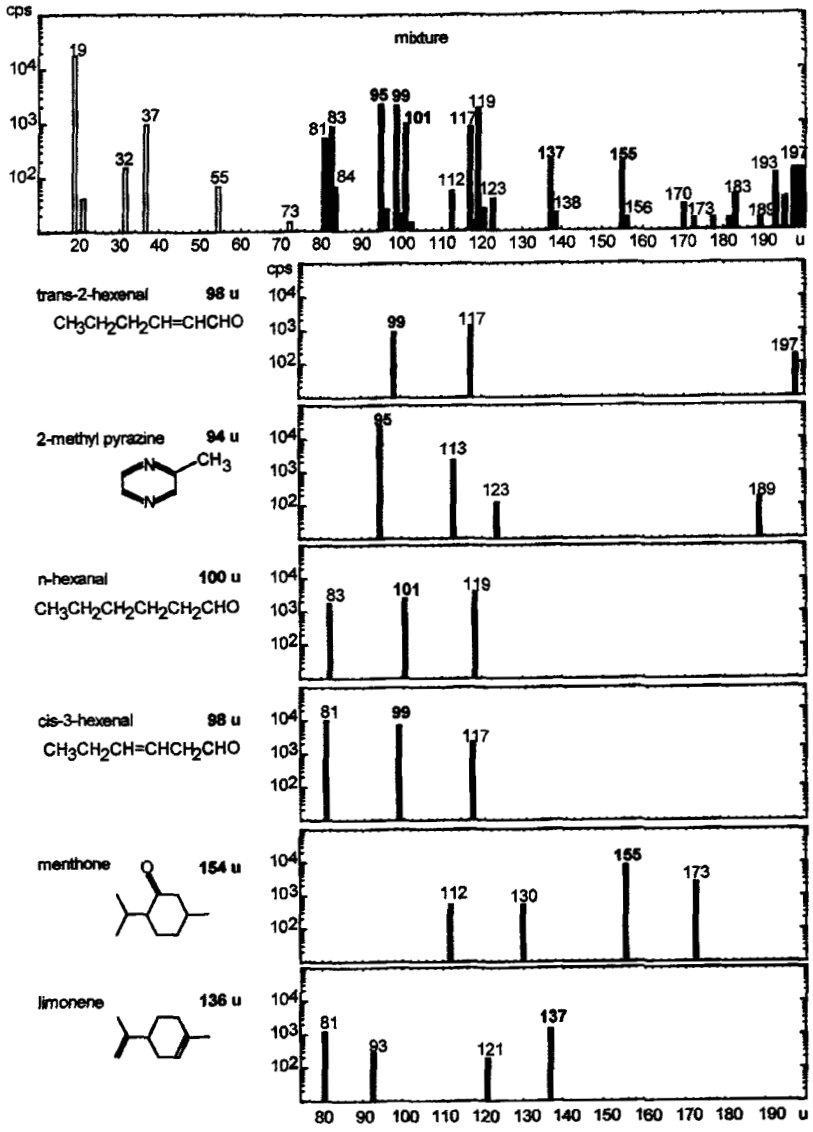

Figure 10. The spectra obtained for the vapour above the six liquid compounds indicated (mostly food flavour compounds) together with their molecular weights. They were obtained by simply holding a small open bottle containing samples of the liquids at the entry port of the SIFT, and again using H_3O^+ and its hydrates as precursor ions. Note the appearance in each spectrum of the protonated parent molecule (molecular weight + 1 u) and their monohydrates, and—in the lower four spectra—fragment ions appear at lower masses, the identifications of which are indicated in the text. The ions at 197 u and 189 u are the proton-bound dimers of the trans-2-hexenal and 2-methyl pyrazine molecules. The spectrum over the wider mass range at the top of this figure, which also indicates the precursor ions (open bars as before), was taken from a bag containing a mixture of all six compounds which indicates that even complex mixtures can be analysed using this SIFT technique.

transfer reactions; this is indicated much earlier for 2-hexenal by equation (4) of this paper. The monohydrates of these ions are also formed, as expected. There is also an impurity at the 1 % level of a species of molecular weight 122 u in the vapour from the 2-methyl pyrazine.

For the second pair of compounds (ii), both the protonated parent molecules (101 u and 99 u respectively) and in each case a second product ion (83 u and 81 u respectively) is seen, the last hydrocarbon ions resulting from the elimination of an H_2O molecule from the protonated parent ion (such is indicated for the 3-hexenal reaction by equation (5*b*) given earlier). The monohydrates of the protonated parent molecules are also seen as expected (119 u and 117 u respectively), but hydration of the hydrocarbon fragment ions is not expected.

The third pair of molecules (iii) apparently partially dissociate in the protonation process. The menthone reaction proceeds thus:

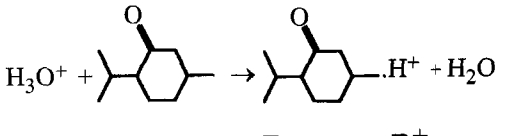

(38*a*)

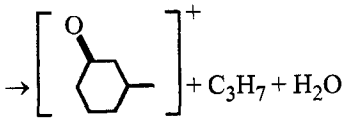

(38*b*)

Here the propyl radical is detached from the cyclohexanone ring in a fraction of the interactions. Notice that the hydrates of both these ions appear on the spectrum (figure 10). However, the limonene reaction is apparently more complex in that four ions above the 5 % level are seen on the spectrum as can be seen in figure 10. The major ion at 137 u is the protonated parent molecule and the larger fragment at 81 u represents the loss of a C_4H_8 moiety thus:

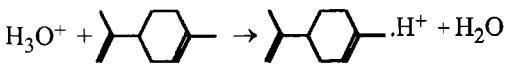

(39*a*)

$$\rightarrow C_6H_9^+ + C_4H_8 + H_2O \qquad (39b)$$

All the products are hydrocarbons and significantly no water hydrates are observed. The minority ion at mass 93 u is very probably protonated toluene and, because we know that this ion does not readily associate a water molecule [11], the ion at 121 u is unlikely to be the hydrate of the 93 u ion. Rather it is probably another fragment of the primary reaction (elimination of a CH_4 moiety?). However, it is possible that the minority ions at 93 u and 121 u are protonated impurity molecules in the sample of limonene.

As a final exercise with these compounds we introduced a sample of each into a single sample bag filled with relatively dry air, thus mixing their vapours, and then looked at the composite vapour with the SIFT. The resultant spectrum (at higher resolution than those in the other six spectra) is also shown in figure 10 over the wider mass range from 10 up to 200 u. Inspection of this spectrum shows that all the ions on the other six spectra are represented and also the ^{13}C isotopic variants of the limonene (at 138 u, a 10 % contribution as expected) and menthone (at 156 u, also about 10 % contribution) are present. Also present are the proton bound dimer ions (e.g. the

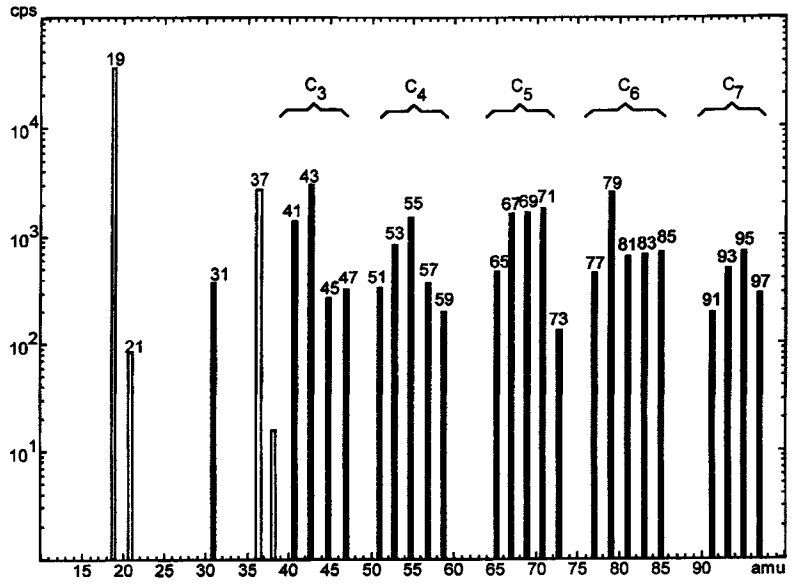

Figure 11. The spectrum obtained in the SIFT, using H_3O^+ precursor ions, of the combustion products of a butane/air flame, obtained by simply immersing a stainless steel capillary connected to the gas entry port of the SIFT into the flame. Note the appearance of the C_3, C_4, C_5, C_6 and C_7 organic compounds which are various hydrocarbons and oxygen-containing organics, presumably aldehydes and ketones. The mass 31 u ion is surely protonated formaldehyde and that at 79 u is probably benzene. The absence of even mass ions indicates that no simple nitrogen-bearing molecules (cyanides and amines) are formed. The gas is also relatively dry and so, as can be seen, the hydrates of H_3O^+ are not so evident as they are in the previous spectra given in this paper.

hexenal dimers at 197 u) and the unsymmetrical dimers (e.g. the proton-bound pyrazine/hexenal ion at 195 u), these being formed in switching reactions between the monohydrates and the other polar molecules present in the mixture of vapours. Note that such spectra could be simplified for analytical purposes by reducing the flow of the air/vapour mixture into the SIFT thus reducing the flow of water vapour into the system and so reducing the fraction of the precursor hydrated hydronium ions. Another approach would be to operate the system (the flow tube and carrier gas) at elevated temperature to inhibit the three-body association reactions that form the hydrated hydronium ions from the H_3O^+ ions (see the review paper [63]), although this diminishes the sensitivity of the system because the carrier gas flow velocity increases with increasing temperature (see the discussion of the technique in §3.2). Alternatively, a flow-drift tube could be used (§6).

5.2. *Combustion: a butane/air flame*

As a final example of the potential of our new technique for the analysis of gases at or near to atmospheric pressure, we have looked at the gases generated in an *n*-butane/air flame (by simply coupling the *n*-butane supply to a Bunsen burner). No attempts were made to control or measure the butane or air flow rates in this very preliminary investigation. The stainless steel entry pipe to the SIFT was immersed in the flame whence some of the combustion products flowed into the apparatus where they reacted with the H_3O^+ ions. (It must be assumed that some of the more condensible combustion products condensed onto the cooler connecting pipes and

hence did not enter the flow tube.) The resultant mass spectrum is startling in its richness as can be seen in figure 11, indicating that a large number of molecules are produced in the combustion process that react with the H_3O^+ ions. Most obvious is the grouping of the ions into C_3, C_4, C_5, C_6 and C_7 compounds which presumably are mostly—but not only—unsaturated hydrocarbons. The lower order saturated hydrocarbons are not protonated by H_3O^+ because of their low proton affinities; these include ethane (C_2H_6), propane (C_3H_8) and butane (C_4H_{10}), and so the ions at 31 u, 45 u and 59 u are not the protonated hydrocarbons but rather they are oxygen-containing organics. The probable identities of these ions are: 31 u, protonated formaldehyde, H_3CO^+; 45 u, protonated acetaldehyde, CH_3CHOH^+; 59 u, protonated acetone, $CH_3COCH_3H^+$. The largest peak in the C_6 group is at 79 u which is very probably protonated benzene. Clearly a very rich chemistry is occurring in this flame. This preliminary experiment indicates the great potential that this new technique has in the investigation of combustion chemistry.

6. Concluding remarks and future directions

We demonstrate in this paper that we have developed a laboratory method of detecting and quantifying many trace gases in atmospheric air and especially on human breath, from samples collected in bags (when longer mass spectrum accumulation times can be used) but significantly also in real time and from a single exhalation of breath. Currently the time response of the SIFT system is only 20 ms, and the detection limit of trace gases for mass spectrum accumulation times of order of 100 s over 100 u is about 10 ppb. For longer accumulation times the sensitivity limit is lowered proportionally. With further research and development, and especially the development of ion sources to produce larger injected currents of the precursor ions (H_3O^+ and O_2^+), we expect to improve the sensitivity limit to well below 1 ppb.

The presence of hydrated hydronium ions along with the H_3O^+ ions is both a blessing and a curse in that these cluster ions provide additional information on the nature of the trace gas molecules but at the same time they complicate the acquired mass spectrum. As we mentioned previously, the fraction of these hydrates can be reduced by operating the carrier gas in the SIFT at higher temperatures, this inhibiting the three-body association reactions that form the hydrate cluster ions [64]. Another approach is to use a small electric drift field along the axis of the flow tube, since it is well-known that the kinetic energy imparted to the ions in this way also slows down three-body association reactions and thus inhibits the formation of cluster ions [64]. However, both the elevated temperature and the drift field approach reduce the reaction time for the ion–molecule reactions that produce the trace gas ions and therefore reduce the sensitivity of this form of detector. This loss of sensitivity in the drift field approach is offset somewhat by the gain in the signal level of the precursor ions that results from the reduced loss of ions by diffusion. We intend to combine the temperature and drift field facility in our next generation of SIFT apparatus for trace gas analysis, to enable us to vary, at will, the fraction of the hydrate ions to the core H_3O^+ ions with all the advantages in analysis that this offers.

A major objective is to carry out several research programmes in collaboration with clinicians, medical physicists and biomedical engineers at Keele University and the North Staffordshire Hospital Trust, to include, for example, the study of indoor and outdoor atmospheric pollutants and their influence on respiratory cells (both *in vitro* and *in vivo*) and on the development of respiratory disease, and the degeneration of lung function by cigarette smoking using trace gas markers for signs of this. Also,

the screening of people in society and patients in hospital will begin for abnormal trace gases on the breath to investigate any connections between certain gases and adverse clinical conditions. We are also collaborating with the food processing industry in the application of our techniques to the 'sniffing' of food products to gauge their degree of 'freshness' and in the development of food flavours. It is clear that the uses of our techniques are numerous; in this paper we have demonstrated their value in medical science, in environmental science, in the fruit and food processing industry, and in combustion chemistry. Our methods are already being used to great effect in these areas and with further development, and especially with the production of a portable device operating on similar principles which we intend to develop, the applications of these techniques will grow rapidly.

Acknowledgments

We are grateful to Peter Rolfe (Keele University), John Thompson (Birmingham University) and Werner Lindinger (Innsbruck University) for stimulating discussions.

References

[1] 1992, *Int. J. Mass Spectrom. Ion Processes*, **118/119**.
[2] 1994, *Int. J. Mass Spectrom. Ion Processes*, **131**.
[3] Eiceman, G. A., 1991, *Critical Reviews in Analytical Chemistry*, **22**, 471.
[4] Lindinger, W., Hirber, J., and Paretzke, H., 1993, *Int. J. Mass Spectrom. Ion Processes*, **129**, 79.
[5] Adams, N. G., Smith, D., and Alge, E., 1980, *J. Phys.* B, **13**, 3235.
[6] Giles, K., Adams, N. G., and Smith, D., 1989, *J. Phys.* B, **22**, 873.
[7] These reactions are now used in a very successful commercial device developed by the company V&F Analyse- und Messtechnik Ges.M.b.H., Andreas-Hofer-Strasse 15, Absam, Austria, for the analysis of a wide range of trace gases in air. Contact person, Dr. Johannes Villinger.
[8] Smith, D., and Adams, N. G., 1987, *Adv. atom. molec. Phys.*, **24**, 1.
[9] Ikezoe, Y., Matsuoka, S., Takebe, M., and Viggiano, A., 1987, *Gas Phase Ion–Molecule Reaction Rate-Constant Through 1986* (Tokyo: Maruzen).
[10] Spanel, P., Pavlik, M., and Smith, D., 1995, *Int. J. Mass Spectrom. Ion Processes*, **145**, 177.
[11] Spanel, P., and Smith, D., 1995, *J. phys. Chem.*, **99**, 15551.
[12] Spanel, P., and Smith, D., 1996, *J. chem. Phys.*, **104**, 1893.
[13] Ferguson, E. E., Fehsenfeld, F. C., and Schmeltekopf, A. L. 1969, *Adv. atom. molec. Phys.*, **5**, 1.
[14] Smith, D., 1992, *Chem. Rev.* **92**, 1473.
[15] Smith, D., and Spanel, P., 1992, *Accts. chem. Res.*, **25**, 414.
[16] Smith, D., and Spanel, P., 1994, *Adv. atom. molec. opt. Phys.*, **32**, 307.
[17] Bohme, D. K., 1975, *Interactions Between Ions and Molecules*, edited by P. Ausloos (New York: Plenum) p. 489.
[18] Su, T., and Chesnavich, W. J., 1982, *J. chem. Phys.*, **76**, 5183.
[19] Mackay, G. I., Lien, M. H., Hopkinson, A. C., and Bohme, D. K., 1978, *Can. J. Chem.*, **56**, 131.
[20] Spanel, P., Smith, D., and Henchman, M. J., 1995, *Int. J. Mass Spectrom. Ion Processes*, **141**, 117.
[21] Mackay, G. I., Tanner, S. T., Hopkinson, A. C., and Bohme, D. K., 1979, *Can. J. Chem.*, **57**, 1518.
[22] Lias, S. G., Bartmess, J. E., Liebman, J. F., Holmes, J. L., Levin, R. D., and Mallard, W. G., 1988, *J. phys. Chem. Ref. Data*, **17** (suppl. 1) and subsequent software updates.
[23] Lide, D. R., editor, 1991, *CRC Handbook of Chemistry and Physics* (Boca Raton: CRC).
[24] Fehsenfeld, F. C., Dotan, I., Albriton, D. L., Howard, C. J., and Ferguson, E. E., 1978, *J. geophys. Res.*, **83**, 1333.

[25] HOPKINSON, A. C., MACKAY, G. I., and BOHME, D. K., 1979, *Can. J. Chem.*, **57**, 2996.
[26] BARTMESS, J. E., 1993, *NIST Negative Ion Energetics Database, Version 3.0*, Standard Reference Database 19B, National Institute of Standards and Technology.
[27] TANNER, S. D., MACKAY, G. I., and BOHME, D. K., 1981, *Can. J. Chem.*, **59**, 1615.
[28] STEWART, J. H., SHAPIRO, R. H., DEPUY, C. H., and BIERBAUM, V. M., 1977, *J. Am. chem. Soc.*, **99**, 7650.
[29] (*a*) DEPUY, C. H., and BIERBAUM, V. M., 1981, *J. Am. chem. Soc.*, **103**, 5034; (*b*) FILLEY, J., DEPUY, C. H., JARROLD, M. F., and BOWERS, M. T., *Ibid.*, **107**, 2818; (*c*) DE KONING, L. J., and NIBBERING, N. M. M., 1987, *ibid.*, **109**, 1715.
[30] (*a*) TAKASHIMA, K., and RIVEROS, J. M., 1978, *J. Am. chem. Soc.*, **100**, 6128; (*b*) GRÜTZMACHER, H. F., and GROTEMEYER, B., 1984, *Org. Mass Spectrom.*, **19**, 135.
[31] KEBARLE, P., SEARLES, S. K., ZOLLA, A., SCARBOROUGH, J., and ARSHADI, M., 1967, *J. Amer. chem. Soc.*, **89**, 6396.
[32] PAYZANT, J. D., YAMDAGNI, R., and KEBARLE, P., 1971, *Can. J. Chem.*, **49**, 3309.
[33] PAYZANT, J. D., CUNNINGHAM, A. D., and KEBARLE, P., 1972, *J. Amer. chem. Soc.*, **94**, 7627.
[34] NARCISI, R. S., and BAILEY, A. D., 1965, *J. geophys. Res.*, **70**, 3687.
[35] SMITH, D., and ADAMS, N. G., 1980, *Topics Current Chem.*, **89**, 1.
[36] KEBARLE, P., 1988, *Techniques for the Study of Ion–Molecule Reactions*, edited by J. M. Farrar and W. H. Saunders Jr. (New York: Wiley), p. 221.
[37] FEHSENFELD, F. C., and FERGUSON, E. E, 1974, *J. chem. Phys.*, **59**, 3181.
[38] YANG, X., ZHANG, X., and CASTLEMAN, A. W., 1991, *Int. J. Mass Spectrom. Ion Processes*, **109**, 339.
[39] SMITH, D., ADAMS, N. G., and HENCHMAN, M. J., 1980, *J. chem. Phys.*, **72**, 4951.
[40] SMITH, D., ADAMS, N. G., and ALGE, E., 1981, *Planet. Space Sci.*, **29**, 449.
[41] WANG YONG, F., and LIFSCHITZ, C., 1995, *Int. J. Mass Spectrom. Ion Processes*, **149/150**, 13.
[42] MCINTOSCH, B. J., ADAMS, N. G., and SMITH, D., 1988, *Chem. Phys. Lett.*, **148**, 142.
[43] BOHME, D. K., MACKAY, G. I., and TANNER, S. D., 1979, *J. Am. chem. Soc.*, **101**, 3724.
[44] FERGUSON, E. E., FEHSENFELD, F. C., and ALBRITTON, D. L., 1979, *Gas Phase Ion Chemistry*, Vol. 1, edited by M. T. Bowers (New York: Academic Press), p. 45.
[45] SMITH, D., ADAMS, N. G., and GRIEF, D., 1977, *J. atmos. terr. Phys.*, **39**, 513.
[46] SMITH, D., ADAMS, N. G., and MILLER, T. M., 1978, *J. chem. Phys.*, **69**, 308.
[47] WILLIAMSON, A. D., and BEAUCHAMP, J. L., 1975, *J. Am. chem. Soc.*, **97**, 5714.
[48] MAYHEW, C. A., and SMITH, D., 1990, *J. Phys.* B, **23**, 3139.
[49] MAYHEW, C. A., and SMITH, D., 1990, *Int. J. Mass. Spectrom. Ion Processes*, **100**, 737.
[50] SEARLES, S. K., and SIECK, L. W., 1970, *J. chem. Phys.*, **53**, 794.
[51] WAYNE, R. P., 1985, *Chemistry of Atmospheres* (Oxford: Clarendon).
[52] LAGG, A., TAUCHER, J., HANSEL, A., and LINDINGER, W., 1994, *Int. J. Mass Spectrom. Ion Processes*, **134**, 55.
[53] KOHLMÜLLER, D., and KOCHEN, W., 1993, *Anal. Biochem.*, **210**, 268.
[54] LUNDBERG, J. O. N., FARKAS-SZALLASI, T., WEITZBERG, E., RINDER, J., LINDHOLM, J., ÄNGGÅRD, A., HÖKFELT, T., LUNDBERG, J. M., and ALVING, K., 1995, *Nature Medicine*, **1**, 370.
[55] SPANEL, P., and SMITH, D. (in preparation).
[56] MANOLIS, A., 1983, *Clin. Chem.*, **29**, 5.
[57] SMITH, D., and SPANEL, P., 1995, *Med. Biol. Eng. Comput.* (submitted).
[58] PHILLIPS, M., 1992, *Sci. Amer.*, July, 52.
[59] PHILLIPS, M., and GREENBERG, J., 1992, *Clin. Chem.*, **38**, 60.
[60] GELMONT, D., STEIN, R. A., and MEAD, J. F., 1981, *Biochem. Biophys. res. Commun.*, **99**, 1456.
[61] JONES, A. W., 1985, *J. anal. Toxicol.*, **9**, 246.
[62] HENCHMAN, M., SMITH, D., and ADAMS, N. G., 1991, *Int. J. Mass Spectrom. Ion Processes*, **109**, 55.
[63] ADAMS, N. G., and SMITH, D., 1983, *Reactions of Small Transient Species*, edited by A. Fontijn and M. A. A. Clyne (London: Academic Press), p. 311.
[64] ADAMS, N. G., and SMITH, D., 1987, *Int. J. Mass Spectrom. Ion Processes*, **8**, 273.